HHS Public Access

Author manuscript

Nature. Author manuscript; available in PMC 2016 September 30.

Published in final edited form as:

Nature. 2016 April 7; 532(7597): 64–68. doi:10.1038/nature17625.

Candidalysin is a fungal peptide toxin critical for mucosal infection

David L. Moyes[1,*], **Duncan Wilson**[2,*,‡], **Jonathan P. Richardson**[1,*], **Selene Mogavero**[2,*], **Shirley X. Tang**[1], **Julia Wernecke**[3,4], **Sarah Höfs**[2], **Remi L. Gratacap**[5], **Jon Robbins**[6], **Manohursingh Runglall**[1,‡‡], **Celia Murciano**[1,‡‡‡], **Mariana Blagojevic**[1], **Selvam Thavaraj**[1], **Toni M. Förster**[2], **Betty Hebecker**[2,7], **Lydia Kasper**[2], **Gema Vizcay**[8], **Simona I. Iancu**[1], **Nessim Kichik**[1,9], **Antje Häder**[10], **Oliver Kurzai**[10], **Ting Luo**[11], **Thomas Krüger**[11], **Olaf Kniemeyer**[11], **Ernesto Cota**[9], **Oliver Bader**[12], **Robert T. Wheeler**[5], **Thomas Gutsmann**[3], **Bernhard Hube**[2,13,14], and **Julian R. Naglik**[1]

[1]Mucosal & Salivary Biology Division, Dental Institute, King's College London, UK

[2]Department of Microbial Pathogenicity Mechanisms, Hans Knöll Institute, Jena, Germany

[3]Research Center Borstel, Division of Biophysics, Borstel, Germany

[4]Deutsches Elektronen-Synchrotron DESY, Hamburg, Germany

[5]Department of Molecular & Biomedical Sciences, University of Maine, Orono, ME, USA

[6]Wolfson CARD, King's College, Guy's Campus, London, UK

[7]Research Group Microbial Immunology, Hans Knöll Institute, Jena, Germany

[8]Centre for Ultrastructural Imaging, King's College London, UK

[9]Department of Life Sciences, Imperial College London, London, UK

[10]Septomics Research Center, Hans-Knöll Institute and Friedrich Schiller University, Jena

[11]Department of Molecular and Applied Microbiology, Hans Knöll Institute, Jena, Germany

[12]Institute for Medical Microbiology, University Medical Center Göttingen, Göttingen, Germany

Correspondence and requests for materials should be addressed to BHu (bernhard.hube@leibniz-hki.de).

*These authors contributed equally to this work.

‡Current address: Aberdeen Fungal Group, School of Medicine, Medical Sciences and Nutrition, University of Aberdeen, Aberdeen, UK

‡‡NIHR Biomedical Research Centre, Guy's and St Thomas' NHS Foundation Trust, London, UK

‡‡‡ERI Biotecmed & Microbiology and Ecology Department, University of Valencia, Valencia, Spain

Supplementary Information is available in the online version of the paper.

Author Contributions DLM, JPR, SXT, MR, CM, MB, SII, NK performed signaling, transcription factor, calcium and cytokine assays, and murine work; DW, SH, SM, TMF, BHe, LK AH, OB and OKu created fungal strains and performed fluorescent microscopy, adhesion, invasion, gene expression and damage assays; RLG and RTW performed zebrafish experiments; JW and TG performed biophysical analysis with artificial membranes; JR performed whole patch clamp analysis; GV performed electron microscopy; ST performed histological analysis; SM, TL, TK and OKn performed LC-MS analyses; JRN, BHu, DLM, JPR and DW wrote the paper; JRN, BHu and EC supervised the project.

The authors declare no competing financial interests.

[13]Friedrich Schiller University, Jena, Germany

[14]Integrated Research and Treatment Center, Center for Sepsis Control and Care, Jena, Germany

Abstract

Cytolytic proteins and peptide toxins are classical virulence factors of several bacterial pathogens which disrupt epithelial barrier function, damage cells and activate or modulate host immune responses. Until now human pathogenic fungi were not known to possess such toxins. Here we identify the first fungal cytolytic peptide toxin in the opportunistic pathogen *Candida albicans*. This secreted toxin directly damages epithelial membranes, triggers a danger response signaling pathway and activates epithelial immunity. Toxin-mediated membrane permeabilization is enhanced by a positively charged C-terminus and triggers an inward current concomitant with calcium influx. *C. albicans* strains lacking this toxin do not activate or damage epithelial cells and are avirulent in animal models of mucosal infection. We propose the name 'Candidalysin' for this cytolytic peptide toxin; a newly identified, critical molecular determinant of epithelial damage and host recognition of the clinically important fungus, *C. albicans*.

Introduction

The ability of mucosal surfaces to discriminate between commensal and pathogenic microbes is essential to human health. The fungus *Candida albicans* is normally a benign member of the human microbiota but is also responsible for millions of mucosal infections each year in immunocompromised hosts, often with severe morbidity[1]. A defining feature of *C. albicans* pathogenesis is the transition from yeast to invasive filamentous hyphae[2]. Hyphae damage mucosal epithelia and induce activation of the activating protein-1 (AP-1) transcription factor c-Fos (via p38-MAPK) and the MAPK phosphatase MKP1 (via ERK1/2-MAPK), which trigger pro-inflammatory cytokine responses[3–7]. These signaling events constitute a 'danger response' against invasive hyphae, thus serving as a sensor of pathogenic *C. albicans* invasion[8–14]. However, it is unclear how *C. albicans* hyphae induce epithelial inflammatory responses and cell damage during mucosal infections. Here we identify and characterize Candidalysin, the first cytolytic peptide toxin isolated from any human fungal pathogen, as the hyphal factor critical for epithelial immune activation and *C. albicans* mucosal infection.

Ece1p is critical for epithelial activation and damage

Despite the well-known association between filamentation and virulence, the molecular mechanism underlying hypha-driven epithelial activation and mucosal damage has remained obscure. To elucidate this mechanism, we screened a panel of *C. albicans* gene deletion mutants that targeted key processes, pathways and proteins known or predicted to be associated with the yeast-hyphal transition and pathogenicity (62 strains). Only hypha-producing strains induced MKP1 phosphorylation (p-MKP1), c-Fos, cytokines (IL-1α, IL-6, G-CSF) and damage in oral epithelial cells (Extended Data Table 1). However, one *C. albicans* mutant (*ece1*Δ/Δ)[15] formed normal hyphae but was incapable of inducing these epithelial danger responses. *C. albicans ECE1* (extent of cell elongation) is highly expressed

by hyphae during epithelial infection (Extended Data Fig. 1a, b) and is predicted to encode a secreted protein[16]. To probe its function we generated a panel of *C. albicans ECE1*mutants (Extended Data Table 2). The *ece1*Δ/Δ strain formed normal hyphae on (Extended Data Fig. 1c), and adhered to and invaded human epithelial cells similarly to wild type *C. albicans* (Extended Data Fig. 1d, e). Indeed, *ece1*Δ/Δ was capable of extensive epithelial invasion, penetrating through multiple epithelial cells (Extended Data Fig. 1f). Despite this, invasive *ece1*Δ/Δ hyphae did not damage epithelia or induce p-MKP1/c-Fos mediated danger responses or cytokine secretion (Fig. 1a–d). Thus, Ece1p is critical for epithelial damage and innate recognition of *C. albicans* hyphae *in vitro*.

Ece1p is critical for mucosal pathogenesis

We next assessed the role of *ECE1* in two *in vivo* models of *C. albicans* mucosal infection. In murine oropharyngeal candidiasis (OPC)[17], mice infected with *C. albicans* wild type or *ECE1* re-integrant (*ece1*Δ/Δ+*ECE1*) strains exhibited disease symptoms, including extensive hyphal invasion of the tongue epithelium, micro-abscesses of infiltrating neutrophils and tissue damage (Fig. 1e, f, h, i). In contrast, tongue tissue from *ece1*Δ/Δ-infected animals (n = 17/20) showed no invasive fungi and no inflammatory infiltrates or damage (Fig. 1g). We detected very low numbers of *ece1*Δ/Δ cells in only 3/20 mice (Extended Data Fig. 2a), which showed no evidence of local epithelial damage (not shown). Quantification of histology sections indicated that the percentage of epithelial surface infected was significantly greater with the wild type and *ECE1* re-integrant strains (Extended DataFig. 2b). In a zebrafish swimbladder model of mucosal infection[18,19], neutrophil recruitment and tissue damage were both significantly lower following *ece1*Δ/Δ infection as compared with the wild type strain (Fig. 1j, k, Extended DataFig. 2c, d). Therefore, *C. albicans* Ece1p is critical for mucosal pathogenesis and is an innate immune activator *in vivo*.

Ece1p encodes a cytolytic peptide toxin

Ece1p is an *in vitro* substrate for Kex2p, a Golgi-located protease that cleaves proteins after lysine-arginine (KR) motifs[20]. Ece1p contains seven KR-processing sites, suggesting it has the potential to produce eight secreted peptides from *C. albicans*[20] (Extended Data Fig. 3a, b). Liquid chromatography – tandem mass spectrometry (LC-MS/MS) analysis confirmed that recombinant Kex2p (rKex2p) processes recombinant Ece1p (rEce1p) and that all eight peptides generated terminated in KR (and fragments thereof, showing that less efficient processing occurs also after a single K or R) (Supplementary information). The importance of Kex2p–mediated Ece1p processing was demonstrated using a *kex2*Δ/Δ null strain[21], which was unable to damage oral epithelia or induce p-MKP1/c-Fos mediated danger responses or cytokine secretion (Extended Data Table 1). To determine which Ece1p peptide(s) were responsible for epithelial activation and damage, oral epithelial cells were incubated with peptides Ece1-I-VIII (1.5 – 70 μM). Only Ece1-III$_{62–93}$ induced p-MKP1, c-Fos, cytokines and damage (Fig. 2a–c, Extended Data Fig. 3c–e). Notably, low Ece1-III$_{62–93}$ concentrations (1.5 – 15 μM) were sufficient to induce c-Fos DNA binding (Fig. 2d), G-CSF and GM-CSF (Fig. 2c, Extended Data Fig. 3c), while high Ece1-III$_{62–93}$ concentrations (70 μM) were required to induce damage (Fig. 2e) and the damage-associated cytokines IL-1α and IL-6, respectively (Extended Data Fig. 3d, e). Ece1-III$_{62–93}$ could also directly lyse multiple human epithelial cell types and induce hemolysis of red blood cells, a classical test

for cytotoxin activity (not shown). Neither the N-terminal hydrophobic region (Ece1-$III_{62–85}$) nor the C-terminal hydrophilic region (Ece1-$III_{86–93}$) induced p-MKP1, c-Fos, cytokines or damage of epithelial cells, either individually or in combination (Extended Data Fig. 3f–h), demonstrating that the peptide containing both regions is required for activity. Therefore, Ece1-$III_{62–93}$ is the active region of Ece1p, acting as an epithelial immune activator and a cytolytic agent.

To confirm that Ece1-$III_{62–93}$ drives epithelial activation and fungal pathogenicity, we generated a *C. albicans* strain lacking only the Ece1-$III_{62–93}$ region (*ece1*Δ/Δ *+ECE1*$_{Δ184–279}$). LC-MS/MS analysis showed that the modified protein in this strain is stable, secreted and processed into each of the predicted peptide fragments, with the exception of the deleted peptide toxin (Supplementary information). Like *ece1*Δ/Δ, *ece1*Δ/Δ *+ECE1*$_{Δ184–279}$ efficiently formed invasive hyphae (not shown). However, *ece1*Δ/Δ *+ECE1*$_{Δ184–279}$ was unable to induce p-MKP1, c-Fos DNA binding, cytokines, or damage epithelia (Extended Fig. 3i–l). In murine OPC, unlike the *ece1*Δ/Δ*+ECE1* complemented strain, *ece1*Δ/Δ*+ECE1*$_{Δ184–279}$-infected mice demonstrated absent (n = 4/10) or low (n = 6/10) fungal burdens, with no evidence of inflammatory infiltrates or local epithelial damage (Fig. 2f–h, Extended Data Fig. 4a and 4b) Likewise, *ece1*Δ/Δ*+ECE1*$_{Δ184–279}$ did not induce full damage in the zebrafish swimbladder model (Fig. 2i, Extended Data Fig. 4c). In contrast, injection of lytic doses of Ece1-$III_{62–93}$ into the swimbladder induced epithelial damage (Fig. 2j, k). Thus, Ece1-$III_{62–93}$ is both necessary and sufficient for epithelial immune activation, damage and mucosal infection *in vivo*.

The amphipathic properties of Ece1-$III_{62–93}$ (SIIGIIMGILGNIPQVIQIIMSIVKAFKGNKR) coupled with the α-helical structure of the N-terminal hydrophobic region (Extended Data Fig. 5a, b) indicated that this fungal peptide may act similarly to cationic antimicrobial peptides and peptide toxins such as melittin[22] (honey bee), magainin 2[23] (African clawed frog) and alamethicin[24] (*Trichoderma viride*). Cytolytic peptide toxins have not previously been found in human pathogenic fungi but bacterial cytolytic toxins are known to induce lesions after binding to target cell membranes[25,26]. To investigate the importance of lipid composition for Ece1-$III_{62–93}$-mediated cytolysis, we used Förster resonance energy transfer (FRET) and electrical impedance spectroscopy to analyze the interactions of Ece1-$III_{62–93}$ with model membranes comprised of lipid bilayers of dioleoylphosphatidylcholine (DOPC) with or without cholesterol. While Ece1-$III_{62–93}$ was able to efficiently intercalate into DOPC membranes (Extended Data Fig. 5c), Ece1-$III_{62–93}$ permeabilization was enhanced in the presence of cholesterol (Fig. 3a,). Ece1-$III_{62–93}$-induced lesions were heterogeneous and transient (Extended Data Fig. 5d), indicating that the peptide may damage target membranes through a ‘carpet-like’ mechanism[27]. Patch-clamp analysis of epithelial cells demonstrated that lesion formation by Ece1-$III_{62–93}$ is rapid and causes an inward current (Fig. 3b), associated with calcium influx (Fig. 3c). Similar phenomena occur with bacterial cytolytic toxins, which are known to trigger cell activation[25,26,28].

We postulated that the positively-charged C-terminal KR residues of Ece1-$III_{62–93}$ might be critical for interacting with negatively-charged components of host membranes to promote lesion formation. Substitution of the KR motif to AA (alanine-alanine; Ece1-$III_{62–93AA}$) did

not affect membrane intercalation (not shown) but significantly reduced the peptide's ability to permeabilize membranes, damage epithelial cells and induce calcium influx (Fig. 3c–e). Thus, the positive C-terminus of Ece1-III$_{62–93}$ is critical for lesion formation and damage induction in epithelial membranes. Notably, Ece1-III$_{62–93AA}$ still induced p-MKP1, c-Fos and the non-damage associated cytokine G-CSF (Extended Data Fig. 5e, f) but not the damage-associated cytokine IL-1α (Fig. 3f), suggesting that Ece1-III$_{62–93AA}$ can be recognized by epithelial immunity without damaging cells. This finding is important as it means that epithelial cells are not only responding to damage but have evolved to specifically recognize the peptide.

Ece1-III$_{62–92K}$ is a secreted cytolytic peptide toxin

To demonstrate that Ece1-III is generated during epithelial infection, we performed LC-MS/MS analysis on the secretome from wild-type *C. albicans* hyphae grown in the presence and absence of epithelial cells (Supplementary information). Notably, Ece1-III was the only peptide detected in the presence of epithelial cells, indicating that the fungus secretes this toxin during mucosal infection. However, the predominant form of secreted Ece1-III terminated in a K residue (SIIGIIMGILGNIPQVIQIIMSIVKAFKGNK; Ece1-III$_{62–92K}$) and not KR (SIIGIIMGILGNIPQVIQIIMSIVKAFKGNKR; Ece1-III$_{62–93KR}$) (Extended Data Table 3). In fungi, it is known that following Kex2p processing, many proteins are subsequently cleaved by Kex1p[29] (also in the Golgi), removing the C-terminal R. LC-MS/MS analysis on the hyphal secretome of a *kex1*Δ/Δ mutant demonstrated that the predominant peptide secreted terminates in KR (not K) (Supplementary information). Therefore, Ece1p is also subject to ordered Kex2p/Kex1p processing. Accordingly, we confirmed that Ece1-III$_{62–92K}$ functioned similarly to Ece1-III$_{62–93KR}$ with respect to epithelial cell activation. Specifically, Ece1-III$_{62–92K}$ is also α-helical (not shown) and induces c-Fos, p-MKP1, cytokines (IL-1α, G-CSF), damage (LDH), membrane intercalation and permeabilization, and calcium influx (Fig 4a–g). Thus, the dominant peptide secreted from *C. albicans* hyphae during mucosal infection is Ece1-III$_{62–92K}$, which acts as a cytolytic peptide toxin that activates epithelial cells.

Based on these data, we propose a model of *C. albicans* mucosal infection whereby invasive hyphae secrete Ece1-$_{62–92K}$ into a membrane-bound 'invasion pocket'[30,31], facilitating peptide accumulation (Extended Data Fig 6). During early stages of infection, sub-lytic concentrations of Ece1-III$_{62–92K}$ induce epithelial immunity by activating the 'danger response' pathway (p-MKP1/c-Fos), alerting the host to the transition from colonizing yeast to invasive, toxin-producing hyphae. As infection progresses, Ece1-III$_{62–92K}$ levels accumulate and elicit direct tissue damage. Mechanistically, we propose that the asymmetric distribution of charge along the α-helix of Ece1-III$_{62–92K}$ facilitates correct peptide orientation relative to the host membrane, enabling intercalation, permeabilization and calcium influx. In conclusion, our data identifies *C. albicans* Ece1-III$_{62–92K}$ as the first cytolytic peptide toxin in a human fungal pathogen and reveals the molecular mechanisms of epithelial damage and host recognition of this clinically important fungus. We propose the name 'Candidalysin' for this newly discovered fungal toxin.

METHODS

Cell lines, reagents and *Candida* strains

Experiments were carried out using the TR146 buccal epithelial squamous cell carcinoma line[32] obtained from the European Collection of Authenticated Cell Cultures (ECACC) and grown in Dulbecco's Modified Eagle's Medium (DMEM, Sigma-Aldrich) supplemented with 10% fetal bovine serum (FBS) and 1% penicillin-streptomycin. Cells were routinely tested for mycoplasma contamination using mycoplasma-specific primers and were found to be negative. Prior to stimulation, confluent TR146 cells were serum-starved overnight, and all experiments were carried out in serum-free DMEM. *C. albicans* wild type strains included the autotrophic strain BWP17+CIp30[33] and the parental strain SC5314[34]. Other *C. albicans* strains used and their sources are listed in Extended Data Tables 1 and 2. *C. albicans* cultures were grown in YPD medium (1% yeast extract, 2% peptone, 2% dextrose) at 30°C overnight. Cultures were washed in sterile PBS and adjusted to the required cell density. Antibodies to phospho-MKP1 and c-Fos were from Cell Signalling Technologies (New England Biolabs UK), mouse anti-human α-actin was from Millipore (UK), and goat anti-mouse and anti-rabbit horseradish peroxidase (HRP)-conjugated antibodies were from Jackson Immunologicals Ltd (Stratech Scientific, UK). Ece1p peptides were synthesized commercially (Proteogenix (France) or Peptide Synthetics (UK).

Generation of *C. albicans ECE1* mutant strains

ECE1 deletion was performed as previously described[35]. Deletion cassettes were generated by PCR[36]. Primers ECE1-FG and ECE1-RG were used to amplify pFA-HIS1 and pFA-ARG4 -based markers. *C. albicans* BWP17[37], was sequentially transformed[38] with the *ECE1*-HIS1 and *ECE1*-ARG4 deletion cassettes and then transformed with CIp10[39], yielding the *ece1*Δ/Δ deletion strain. For complementation, the *ECE1* gene plus upstream and downstream intergenic regions were amplified with primers ECE1-RecF3k and ECE1-RecR and cloned into plasmid CIp10 at *Mlu*I and *Sal*I sites. This plasmid was transformed into the uridine auxotrophic *ece1*Δ/Δ strain, yielding the *ece1*Δ/Δ+*ECE1* complemented strain. For generation of the *ece1*Δ/Δ+$ECE1_{\Delta 184–279}$ strain, the CIp10-*ECE1* was amplified with primers Pep3-F1 and Pep3-R1, digested with ClaI and re-ligated, yielding the CIp10+$ECE1_{\Delta 184–279}$ plasmid. This plasmid was transformed into the uridine auxotrophic *ece1*Δ/Δ strain, yielding the *ece1*Δ/Δ+$ECE1_{\Delta 184–279}$ strain. All integrations were confirmed by PCR/sequencing and at least two independent isogenic transformants were created to confirm results. *KEX1* deletion was performed exactly as the *ECE1* deletion but using primers KEX1-FG and KEX1-RG for creating the deletion cassette. Fluorescent strains of *ece1*Δ/Δ and BWP17 were constructed as previously described[40]. Briefly, the *ece1*Δ/Δ and BWP17 strains were transformed with the pENO1-dTom-NATr plasmid. Primers used to clone and construct the *ECE1* genes and intragenic regions are listed in Extended Data Table 4. Strains are listed in Extended Data Table 2.

Construction of *C. albicans ECE1* promoter-GFP strain

ECE1 promoter (primers 5′*ECE1*prom-NarI / 3′*ECE1*prom-XhoI) and terminator (5′*ECE1*term-SacII / 5′*ECE1*term-SacI) were amplified and cloned into pADH1-GFP. Resulting pSK-p*ECE1*-GFP was verified by sequencing. *C. albicans* SC5314 was

transformed with the *pECE1-GFP* transformation cassette[38]. Resistance to nourseothricin was used as selective marker and correct integration of GFP into the *ECE1* locus was verified by PCR. Primers for cloning and validation are listed in Extended Data Table 4. Strains are listed in Extended Data Table 2.

RNA isolation and real-time PCR analysis

C. albicans cells grown on TR146 epithelial cells were collected into RNA pure (PeqLab), centrifuged and the pellet resuspended in 400 μl AE buffer (50 mM Na-acetate pH 5.3, 10 mM EDTA, 1% SDS). Samples were vortexed (30 s), and an equal volume of phenol/chloroform/isoamyl alcohol (25:24:1) was added and incubated for 5 min (65°C) before subjected to 2x freeze-thawing. Lysates were clarified by centrifugation and the RNA precipitated with isopropyl alcohol/0.3 M sodium acetate by incubating for 1 h at −20°C. Precipitated pellets were washed (2× 1 ml 70% ice-cold ethanol), resuspended in DEPC-treated water and stored at −80°C. RNA integrity and concentration was confirmed using a Bioanalyzer (Agilent). RNA (500 ng) was treated with DNase (Epicenter) and cDNA synthesized using Reverse Transcriptase Superscript III (Invitrogen). cDNA samples were used for qPCR with EVAgreen mix (Bio&Sell). Primers (ACT1-F and ACT1-R for actin, ECE1-F and ECE1-R for *ECE1* - Extended Data Table 4) were used at a final concentration of 500 nM. qPCR amplifications were performed using a Biorad CFX96 thermocycler. Data was evaluated using Bio-Rad CFX Manager 3.1 (Bio-Rad) with *ACT1* as the reference gene and t_0 as the control sample.

Western blotting

TR146 cells were lysed using a modified RIPA lysis buffer (50 mM Tris-HCl pH 7.4, 150 mM NaCl, 1 mM EDTA, 1% Triton X-100, 1% sodium deoxycholate, 0.1% SDS) containing protease (Sigma-Aldrich) and phosphatase (Perbio Science) inhibitors[41], left on ice (30 min) and then clarified (10 min) in a refrigerated microfuge. Lysate total protein content was determined using the BCA protein quantitation kit (Perbio Science). 20 μg of total protein was separated on 12% SDS-PAGE gels before transfer to nitrocellulose membranes (GE Healthcare). After probing with primary (1:1000) and secondary (1:10,000) antibodies, membranes were developed using Immobilon chemiluminescent substrate (Millipore) and exposed to X-Ray film (Fuji film). Human α-actin was used as a loading control.

Transcription factor DNA binding assay

DNA binding activity of transcription factors was assessed using the TransAM transcription factor ELISA system (Active Motif) as previously described[41,42]. Serum-starved TR146 epithelial cells were treated for 3 h before being differentially lysed to recover nuclear proteins using a nuclear protein extraction kit (Active Motif) according to the manufacturer's protocol. Protein concentration was determined (BCA protein quantitation kit (Perbio Science)) and 5 μg of nuclear extract was assayed in the TransAM system according to the manufacturer's protocol. Data was expressed as fold-change in A_{450nm} relative to resting cells.

Cytokine determination

Cytokine levels in cell culture supernatants were determined using the Performance magnetic Fluorokine MAP cytokine multiplex kit (Bio-techne) and a Bioplex 200 machine. The data were analyzed using Bioplex Manager 6.1 software to determine analyte concentrations.

Cell damage assay

Following incubation, culture supernatant was collected and assayed for lactate dehydrogenase (LDH) activity using the Cytox 96 Non-Radioactive Cytotoxicity Assay kit (Promega) according to the manufacturer's instructions. Recombinant porcine LDH (Sigma-Aldrich) was used to generate a standard curve.

Epithelial adhesion assay

Quantification of *C. albicans* adherence to TR146 epithelial cells was performed as described previously[43]. Briefly, TR146 cells were grown to confluence on glass coverslips for 48 h in tissue culture plates in DMEM medium. *C. albicans* yeast cells (2×10^5) were added into 1 ml serum-free DMEM, incubated for 60 min (37°C/5% CO_2) and non-adherent *C. albicans* cells removed by aspiration. Following washing (3× 1 ml PBS), cells were fixed with 4% paraformaldehyde (Roth) and adherent *C. albicans* cells stained with Calcofluor White and quantified using fluorescence microscopy. The number of adherent cells was determined by counting 100 high power fields of 200 μm × 200 μm size. Exact total cell numbers were calculated based on the quantified areas and the total size of the cover slip.

Epithelial invasion assay

C. albicans invasion of epithelial cells was determined as described previously[43]. Briefly, TR146 epithelial cells were grown to confluence on glass coverslips for 48 h and then infected with *C. albicans* yeast cells (1×10^5), for 3 h in a humidified incubator (37°C/5% CO_2). Following washing (3x PBS), the cells were fixed with 4% paraformaldehyde. All surface adherent fungal cells were stained for 1 h with a rabbit anti-*Candida* antibody and subsequently with a goat anti-rabbit-Alexa Fluor 488 antibody. After rinsing with PBS, epithelial cells were permeabilized (0.1% Triton X-100 in PBS for 15 min) and fungal cells (invading and non-invading) were stained with Calcofluor White. Following rinsing with water, coverslips were visualized using fluorescence microscopy. The percentage of invading *C. albicans* cells was determined by dividing the number of (partially) internalized cells by the total number of adherent cells. At least 100 fungal cells were counted on each coverslip.

Imaging of *C. albicans* growth and invasion of epithelial cells

TR146 cells (10^5/ml) seeded on glass coverslips in DMEM/10% FBS were infected with *C. albicans* (2.5×10^4 cfu/ml) in DMEM and incubated for 6 h (37°C/5% CO_2). Cells were washed with PBS, fixed overnight (4°C in 4% paraformaldehyde) and stained with Concanavalin A-Alexa Fluor 647 in PBS (10 μg/ml) for 45 min at room temperature in the dark with gentle shaking (70 rpm) to stain the fungal cell wall. Epithelial cells were permeabilised with 0.1% Triton X-100 for 15 min at 37°C in the dark, then washed and stained with 10 μg/ml Calcofluor White (0.1 M Tris-HCl pH 9.5) for 20 min at room

temperature in the dark with gentle shaking. Cells were rinsed in water and mounted on slides with 6 μl of ProLong Gold anti-fade reagent, before air drying for 2 h in the dark. Fluorescence microscopy was performed on a Zeiss Axio Observer Z1 microscope, and 5 phase images were taken per picture.

Scanning Electron Microscopy

For scanning electron microscopy (SEM) analysis, TR146 cells were grown to confluence on Transwell inserts (Greiner) and serum starved overnight in serum-free DMEM. After 5 h of *C. albicans* incubation on epithelial cells at an MOI of 0.01, cell media was removed and samples were fixed overnight at 4°C with 2.5% (v/v) glutaraldehyde in 0.05 M HEPES buffer (pH 7.2) and post-fixed in 1% (w/v) osmium tetroxide for 1 h at room temperature. After washing, samples were dehydrated through a graded ethanol series before being critical point dried (Polaron E3000, Quorum Technologies Ltd). Dried samples were mounted using carbon double side sticky discs (TAAB) on aluminium pins (TAAB) and gold coated in an Emitech K550X sputter coater (Quorum Technologies Ltd). Samples were examined and images recorded using a FEI Quanta 200 field emission scanning electron microscope operated at 3.5 kV in high vacuum mode.

Zebrafish swimbladder mucosal infection model

Zebrafish infections were performed in accordance with NIH guidelines under Institutional Animal Care and Use Committee (IACUC) protocol A2009-11-01 at the University of Maine. To determine sample size, a power calculation was done for all experiments based on 2-tails T-test in order to detect a minimum effect size of 0.8, with an alpha error probability of 0.05 and a power (1 – beta error probability) of 0.95. This gave a minimum number of 42 fish for each group. The fish selected for the experiments were randomly assigned to the different groups by picking them from a pool without bias and the groups were injected in different orders. No blinding was used to read the results. Ten to twenty zebrafish per group per experiment were maintained at 33°C in E3 + PTU and used as previously described[40]. Briefly, 4 day post-fertilization (dpf) larvae were treated with 20 μg/ml dexamethasone dissolved in 0.1% DMSO 1 h prior to infection and thereafter. For tissue damage and neutrophil recruitment, individual AB or *mpo:GFP* fish (respectively) were injected into the swimbladder with 4 nl of PBS with/without 25–40 *C. albicans* yeast cells of *ece1*Δ/Δ-*dTomato*, *ece1*Δ/Δ+*ECE1*+*dTomato*, *ece1*Δ/Δ+*ECE1*$_{\Delta 184–279}$+*dTomato* or BWP17-*dTomato*. For tissue damage, 1 nl of Sytox green (0.05 mM in 1% DMSO) was injected at 20 h post-infection into the swimbladder and fish were imaged by confocal microscopy at 24 h post-infection. For neutrophil recruitment, fish were imaged at 24 h post-injection. For synthetic peptide damage, AB or α-catenin:citrine[44] fish were injected with 2 nl of peptide (9 ng or 1.25 ng per fish) or vehicle (40% DMSO or 5% DMSO) + SytoxGreen (0.05 mM in 1% DMSO) or SytoxOrange (0.5 mM in 10% DMSO) and the fish imaged by confocal microscopy 4 h later. Numbers of neutrophils and damaged cells observed were counted and tabulated for each fish.

Zebrafish swimbladder fluorescence microscopy

Live zebrafish imaging was carried out as previously described[40]. Briefly, fish were anesthetized in Tris-buffered Tricaine (200 μg/ml, Western Chemicals) and further

immobilized in a solution of 0.4% low-melting-point agarose (LMA, Lonza) in E3 + Tricaine in a 96-well plate glass-bottom imaging dish (Greiner Bio-On). Confocal imaging was carried out using an Olympus IX-81 inverted microscope with an FV-1000 laser scanning confocal system (Olympus). Images were collected and processed using Fluoview (Olympus) and Photoshop (Adobe Systems Inc.). Panels are either a single slice for the differential interference contrast channel (DIC) with maximum projection overlays of fluorescence image channels (red-green), or maximum projection overlays of fluorescence channels. The number of slices for each maximum projection is specified in the legend of individual figures.

Murine oropharyngeal candidiasis model

Murine infections were performed under UK Home Office Project Licence PPL 70/7598 in dedicated animal facilities at King's College London. No statistical method was used to predetermine sample size. No method of randomization was used to allocate animals to experimental groups. Mice in the same cage were part of the same treatment. The investigators were not blinded during outcome assessment. A previously described murine model of oropharyngeal candidiasis using female Balb/c mice[45] was modified for investigating early infection events. Briefly, mice were treated sub-cutaneously with 3 mg/mouse (in 200 μl PBS with 0.5% Tween 80) of cortisone acetate on days −1 and 1 post-infection. On day 0, mice were sedated for ~75 min with an intra-peritoneal injection of 110 mg/kg ketamine and 8 mg/kg xylazine, and a swab soaked in a 10^7 cfu/ml *C. albicans* yeast culture in sterile saline was placed sub-lingually for 75 min. After 2 days, mice were sacrificed, the tongue excised and divided longitudinally in half. One half was weighed, homogenized and cultured to derive quantitative *Candida* counts. The other half was processed for histopathology and immunohistochemistry.

Immunohistochemistry of murine tissue

C. albicans infected murine tongues were fixed in 10% (v/v) formal-saline before being embedded and processed in paraffin wax using standard protocols. For each tongue, 5 μm sections were prepared using a Leica RM2055 microtome and silane coated slides. Sections were dewaxed using xylene, before *C. albicans* and infiltrating inflammatory cells were visualized by staining using Periodic Acid-Schiff (PAS) stain and counterstaining with haematoxylin. Sections were then examined by light microscopy. Histological quantification of infection was undertaken by measuring the area of infected epithelium and expressed as a percentage relative to the entire epithelial area.

Whole cell patch clamp

TR146 epithelial cells were grown in 35 mm petri dishes (Nunc) for 48 h before recordings at low cell density (10–30% confluence). Cells were superfused with a modified Krebs solution (120 mM NaCl, 3 mM KCl, 2.5 mM $CaCl_2$, 1.2 mM $MgCl_2$, 22.6 mM $NaHCO_2$, 11.1 mM glucose, 5 mM HEPES pH 7.4). Isolated cells were recorded at room temperature (21–23°C) in whole cell mode using microelectrodes (5–7 MΩ) containing 90 mM potassium acetate, 20 mM KCl, 40 mM HEPES, 3 mM EGTA, 3 mM $MgCl_2$, 1 mM $CaCl_2$ (free Ca^{2+} 40 nM), pH 7.4. Cells were voltage clamped at −60 mV using an Axopatch 200A amplifier (Axon Instruments) and current/voltage curves were generated by 1 s steps

between −100 to + 50 mV. Treatments were applied to the superfusate to produce the final required concentration, with vehicle controls similarly applied. Data was recorded using Clampex software (PClamp 6, Axon Instrument) and analyzed with Clampfit 10.

Calcium flux

TR146 cells were grown in a 96-well plate overnight until confluent. The medium was removed and 50 μl of a Fura-2 solution (5 μl Fura-2 (Life Technologies)(2.5 mM in 50% Pluronic F-127 (Life technologies):50% DMSO), 5 μl probenecid (Sigma) in 5 ml saline solution (NaCl (140 mM), KCl (5 mM), $MgCl_2$ (1 mM), $CaCl_2$ (2 mM), Glucose (10 mM) and HEPES (10 mM), adjusted to pH 7.4)) was added and the plate incubated for 1 h at 37°C/5% CO_2. The Fura-2 solution was replaced with 50 μl saline solution and baseline fluorescence readings (excitation 340 nm/emission 520nm) taken for 10 min using a FlexStation 3 (Molecular Devices). Ece1 peptides were added at different concentrations and readings immediately taken for up to 3 h. The data was analyzed using Softmax Pro software to determine calcium present in the cell cytosol and expressed as the ratio between excitation and emission spectra.

Impedance spectroscopy of tethered bilayer lipid membranes (tBLMs)

tBLMs with 10% tethering lipids and 90% spacer lipids (T10 slides) were formed using the solvent exchange technique[46,47] according to the manufacturer's instructions (SDx Tethered Membranes Pty Ltd, Sydney, Australia). Briefly, 8 μl of 3 mM lipid solutions in ethanol were added, incubated for 2 min and then 93.4 μl buffer (100 mM KCl, 5 mM HEPES, pH 7.0) was added. After rinsing 3x with 100 μl buffer the conductance and capacitance of the membranes were measured for 20 min before injection of Ece1 peptides at different concentrations. All experiments were performed at room temperature. Signals were measured using the tethaPod (SDx Tethered Membranes Pty Ltd, Sydney, Australia).

FRET intercalation experiments

Intercalation of Ece1 peptides into phospholipid liposomes was determined by FRET spectroscopy applied as a probe-dilution assay[48]. Phospholipids mixed with each 1% (mol/mol) of the donor dye NBD-phosphatidylethanolamine (NBD-PE) and of the acceptor dye rhodamine-PE, were dissolved in chloroform, dried, solubilized in 1 ml buffer (100 mM KCl, 5 mM HEPES, pH 7.0) by vortexing, sonicated with a titan tip (30 W, Branson sonifier, cell disruptor B15), and subjected to three cycles of heating to 60°C and cooling down to 4°C, each for 30 min. Lipid samples were stored at 4°C for at least 12 h before use. Ece1 peptide was added to liposomes and intercalation was monitored as the increase of the quotient between the donor fluorescence intensity I_D at 531 nm and the acceptor intensity I_A at 593 nm (FRET signal) independent of time.

Circular Dichroism spectroscopy

CD measurements were performed using a Jasco J-720 spectropolarimeter (Japan Spectroscopic Co., Japan), calibrated as described previously[49]. CD spectra represent the average of four scans obtained by collecting data at 1 nm intervals with a bandwidth of 2

nm. The measurements were performed in 100 mM KCl, 5 mM HEPES, pH 7.0 at 25°C and 40°C in a 1.0 mm quartz cuvette. The Ece1-III concentration was 15 μM.

Planar lipid bilayers

Planar lipid bilayers were prepared using the Montal-Mueller technique[50] as described previously[51]. All measurements were performed in 5 mM HEPES, 100 mM KCl, pH 7.0 (specific electrical conductivity 17.2 mS/cm) at 37°C.

Hyphal secretome preparation for LC-MS/MS analysis

Candida strains were cultured for 18 h in hyphae inducing conditions (YNB medium containing 2% sucrose, 75 mM MOPSO buffer pH 7.2, 5 mM N-acetyl-D-glucosamine, 37°C). Hyphal supernatants were collected by filtering through a 0.2 μm PES filter, and peptides were enriched by Solid Phase Extraction (SPE) using first C4 and subsequently C18 columns on the C4 flowthrough. After drying in a vacuum centrifuge, samples were resolubilised in loading solution (0.2% formic acid in 71:27:2 ACN/H_2O/DMSO (v/v/v)) and filtered through a 10 kDa MWCO filter. The filtrate was transferred into HPLC vials and injected into the LC-MS/MS system. LC-MS/MS analysis was carried out on an Ultimate 3000 nano RSLC system coupled to a QExactive Plus mass spectrometer (ThermoFisher Scientific). Peptide separation was performed based on a direct injection setup without peptide trapping using an Accucore C4 column as stationary phase and a column oven temperature of 50°C. The binary mobile phase consisting of A) 0.2% (v/v) formic acid in 95:5 H_2O/DMSO (v/v) and B) 0.2% (v/v) formic acid in 85:10:5 ACN/H_2O/DMSO (v/v/v) was applied for a 60 min gradient elution: 0–1.5 min at 60% B, 35–45 min at 96% B, 45.1–60 min at 60% B. The Nanospray Flex Ion Source (ThermoFisher Scientific) provided with a stainless steel emitter was used to generate positively charged ions at 2.2 kV spray voltage. Precursor ions were measured in full scan mode within a mass range of m/z 300–1600 at a resolution of 70k FWHM using a maximum injection time of 120 ms and an automatic gain control target of 1e6. For data-dependent acquisition, up to 10 most abundant precursor ions per scan cycle with an assigned charge state of z = 2–6 were selected in the quadrupole for further fragmentation using an isolation width of m/z 2.0. Fragment ions were generated in the HCD cell at a normalised collision energy of 30 V using nitrogen gas. Dynamic exclusion of precursor ions was set to 20 s. Fragment ions were monitored at a resolution of 17.5k (FWHM) using a maximum injection time of 120 ms and an AGC target of 2e5.

Protein database search

Thermo raw files were processed by the Proteome Discoverer (PD) software v1.4.0.288 (Thermo). Tandem mass spectra were searched against the Candida Genome Database (http://www.candidagenome.org/download/sequence/C_albicans_SC5314/Assembly22/current/C_albicans_SC5314_A22_current_orf_trans_all.fasta.gz;status: 2015/05/03) using the Sequest HT search algorithm. Mass spectra were searched for both unspecific cleavages (no enzyme) and tryptic peptides with up to 4 missed cleavages. The precursor mass tolerance was set to 10 ppm and the fragment mass tolerance to 0.02 Da. Target Decoy PSM Validator node and a reverse decoy database was used for (qvalue) validation of the peptide spectral matches (PSMs) using a strict target false discovery (FDR) rate of < 1%. Furthermore, we used the Score versus Charge State function of the Sequest engine to filter

out insignificant peptide hits (xcorr of 2.0 for z=2, 2.25 for z=3, 2.5 for z=4, 2.75 for z=5, 3.0 for z=6). At least two unique peptides per protein were required for positive protein hits.

Statistics

TransAM and patch clamp data were analyzed using a paired t-test whilst cytokines, LDH and calcium influx data were analyzed using one-way ANOVA with all compared groups passing an equal variance test. Murine *in vivo* data was analyzed using the Mann-Whitney test. Zebrafish data was analyzed using the Kruskal-Wallis test with Dunn's multiple comparison correction. In all cases, $P < 0.05$ was taken to be significant.

Extended Data

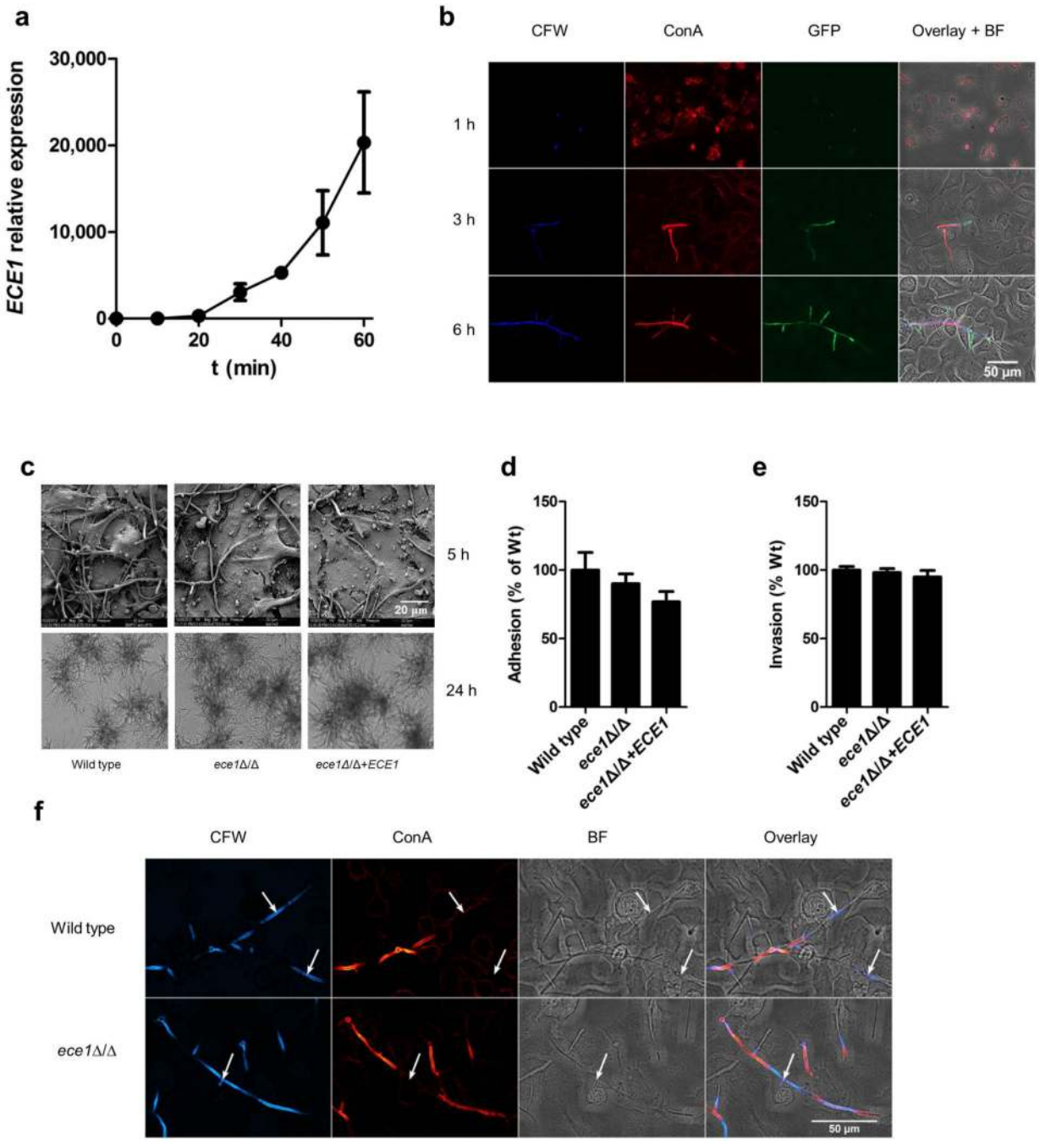

Extended Data Figure 1. *C. albicans ECE1* expression and phenotypic effects of *ECE1* gene deletion

(a) Relative expression (vs t = 0) of *ECE1* in *C. albicans* wild type over time after addition of yeast cells to TR146 epithelial cells as measured by RT-qPCR. **(b)** Imaging confirmation of *ECE1* expression over time within *C. albicans* wild type. *C. albicans* cells expressing GFP under the control of the *ECE1* 5′ intragenic region, containing the *ECE1* promoter, were grown on TR146 epithelial cells and stained with calcofluor white (CFW, post-

permeabilization) to show cell wall chitin and Alexa-Fluor-647-labelled concanavalin A (ConA, pre-permeabilization) to show carbohydrates. A composite image showing CFW, ConA, GFP and the brightfield (BF) image is shown. **(c)** Scanning electron micrographs (top panels, 5 h) and light microscopy (bottom panels, 24 h) showing no gross abnormalities in hypha formation between *C. albicans* wild type (BWP17+CIp30), *ECE1*-deletion (*ece1*Δ/Δ) and *ECE1* re-integrant (*ece1*Δ/Δ+*ECE1*) strains after infection of TR146 epithelial cells. **(d)** No difference in adhesion of *C. albicans* wild type, *ece1*Δ/Δ and *ece1*Δ/Δ+*ECE1* strains to TR146 epithelial cells after 60 min. **(e)** No difference in invasion of *C. albicans* wild type, *ece1*Δ/Δ and *ece1*Δ/Δ+*ECE1* strains into TR146 epithelial cells after 3 h. **(f)** Fluorescence staining of *C. albicans* wild type and *ece1*Δ/Δ hyphae invading through TR146 epithelial cells. Fungal cells are stained with calcofluor white (CFW, post-permeabilization) and Alexa-Fluor-647-labelled concanavalin A (ConA, pre-permeabilization) to show cell wall chitin and carbohydrates, respectively, and to distinguish between invading hyphae (only stained after permeabilization) and non-invading hyphae (stained both pre- and post-permeabilization). Levels of chitin and β-glucan are comparable in both strains. White arrows indicate invasion into epithelial cells. Data shown are representative **(b, c, f)** or the mean **(a, d, e)** of three biological replicates. Error bars show ± SEM.

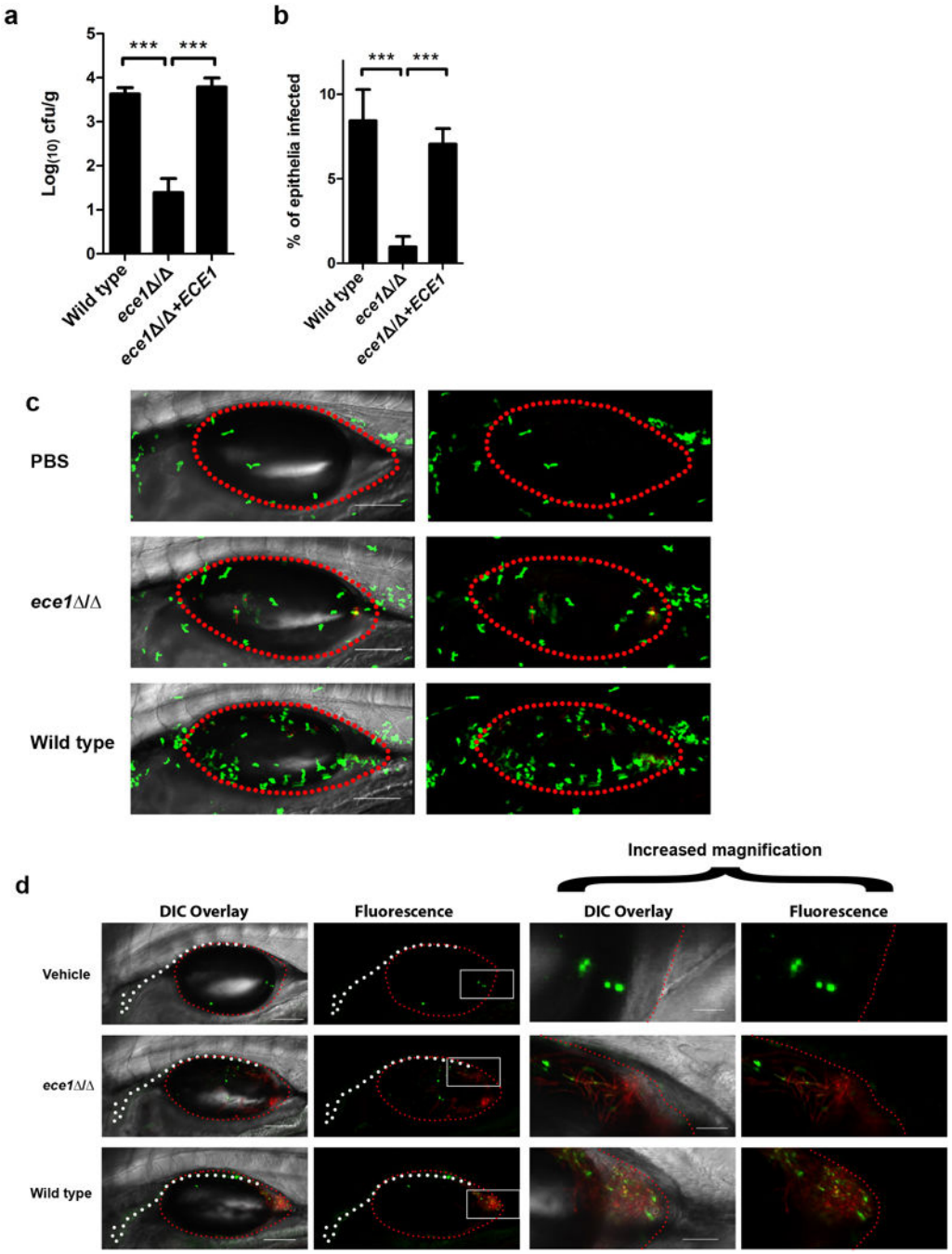

Extended Data Figure 2. ***C. albicans*** **Ece1p is critical for mucosal virulence** ***in vivo***

(a) Fungal burdens recovered from the tongues of mice infected with *C. albicans* wild type (BWP17+CIp30) (n (number of mice) = 13), *ECE1*-deletion (*ece1Δ/Δ*) (n = 20) and *ECE1* re-integrant (*ece1Δ/Δ+ECE1*) (n = 24) strains after 2 day oropharyngeal infection. **(b)** Average percentage of the entire tongue epithelium area infected in different groups of mice infected with the different *C. albicans* strains. **(c)** Confocal imaging of 4 day post-fertilization (dpf) *mpo-gfp* transgenic zebrafish swimbladders infected with *C. albicans* wild type (BWP17+CIp30*+dTomato*), *ECE1*-deletion (*ece1Δ/Δ+dTomato*) and *ECE1* re-integrant

(*ece1Δ/Δ+ECE1+dTomato*) strains for 24 h. *C. albicans* cells appear red whilst neutrophils appear green. Red dots outline the swimbladder. Images are composites of maximum projections in the red and green channels (25 slices each, approximately 100 μm depth) with (left) or without (right) a single slice in the DIC channel overlay. Scale bars represent 100 μm. **(d)** Confocal imaging of 4 dpf zebrafish swimbladders infected with *C. albicans* wild type (BWP17+CIp30*+dTomato*), *ECE1*-deletion (*ece1Δ/Δ+dTomato*) and *ECE1* re-integrant (*ece1Δ/Δ+ECE1+dTomato*) strains for 24 h stained with the fluorescent exclusion dye Sytox Green. *C. albicans* cells appear red and damaged epithelial cells appear green. White dots outline the pronephros and red dots outline the swimbladder. Images are composites of maximum projections in the red and green channels (25 slices each, approximately 100 μm depth) with (left) or without (right) a single slice in the DIC channel overlay. High magnification images of the white boxes are shown. Scale bars (bottom right) represent 100 μm (low magnification) and 30 μm (high magnification). Data shown are the mean **(a, b)** or representative **(c, d)** of at least three biological replicates. Error bars show ± SEM. Data were analyzed by Mann-Whitney test. *** = $P < 0.001$.

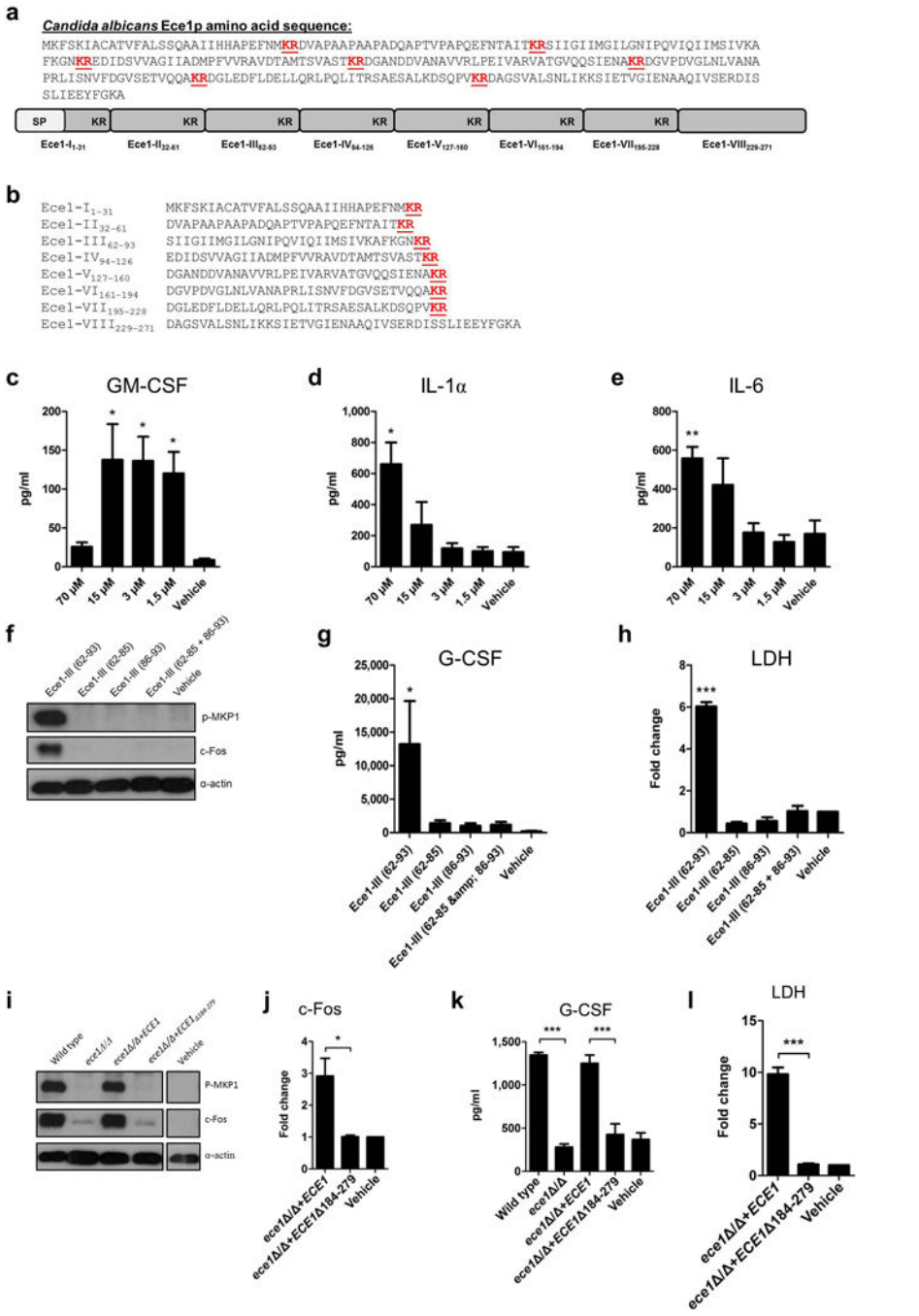

Extended Data Figure 3. Ece1-III$_{62–93}$ is the active region of Ece1p

(a) Amino acid sequence of Ece1p and a schematic of the protein, indicating the signal peptide (SP), lysine-arginine motifs (KR) at the C-terminus of each peptide, and the processed peptides (Ece1-I-VIII) produced by Kex2p cleavage. **(b)** Amino acid sequences of the processed peptides (Ece1-I-VIII) produced by Kex2p cleavage. Induction of **(c)** GM-CSF, **(d)** IL-1α and **(e)** IL-6 secreted after stimulation of TR146 epithelial cells for 24 h with varying concentrations of Ece1-III$_{62–93}$ (70 μM - 1.5 μM). **(f)** Phosphorylation of MKP-1 and c-Fos production after 2 h treatment of TR146 epithelial cells with 15 μM of Ece1-

$III_{62–85}$ (hydrophobic region), Ece1-$III_{86–93}$ (hydrophillic region), Ece1-$III_{62–85}$ and Ece1-$III_{86–93}$ together, or Ece1-$III_{62–93}$ alone. **(g)** Induction of G-CSF secretion after 24 h treatment of TR146 epithelial cells with 15 μM of Ece1-$III_{62–85}$, Ece1-$III_{86–93}$, Ece1-$III_{62–85}$ and Ece1-$III_{86–93}$ together, or Ece1-$III_{62–93}$ alone. **(h)** Fold change induction of LDH release after 24 h treatment of TR146 epithelial cells with 70 μM of Ece1-$III_{62–85}$, Ece1-$III_{86–93}$, Ece1-$III_{62–85}$ and Ece1-$III_{86–93}$ together, or Ece1-$III_{62–93}$ alone. **(i)** Induction of p-MKP-1 and c-Fos 2 h post-infection (p.i.) with the indicated *C. albicans* strains (MOI = 10). **(j)** c-Fos DNA binding induction 3 h p.i. with indicated *C. albicans* strains (MOI = 10). **(k)** G-CSF secretion and **(l)** LDH release 24 h p.i. with indicated *C. albicans* strains (MOI = 0.01). Data shown are representative **(f, i)** or the mean **(c-e, g-h, j-l)** of three biological replicates. Error bars show ± SEM. Data were analyzed by one-way ANOVA (**c-e, g-h,k-l**) or T test (**j**). * = $P < 0.05$, ** = $P < 0.01$, *** = $P < 0.001$ (compared with vehicle control). For gel source data, see Supplementary Figure 1.

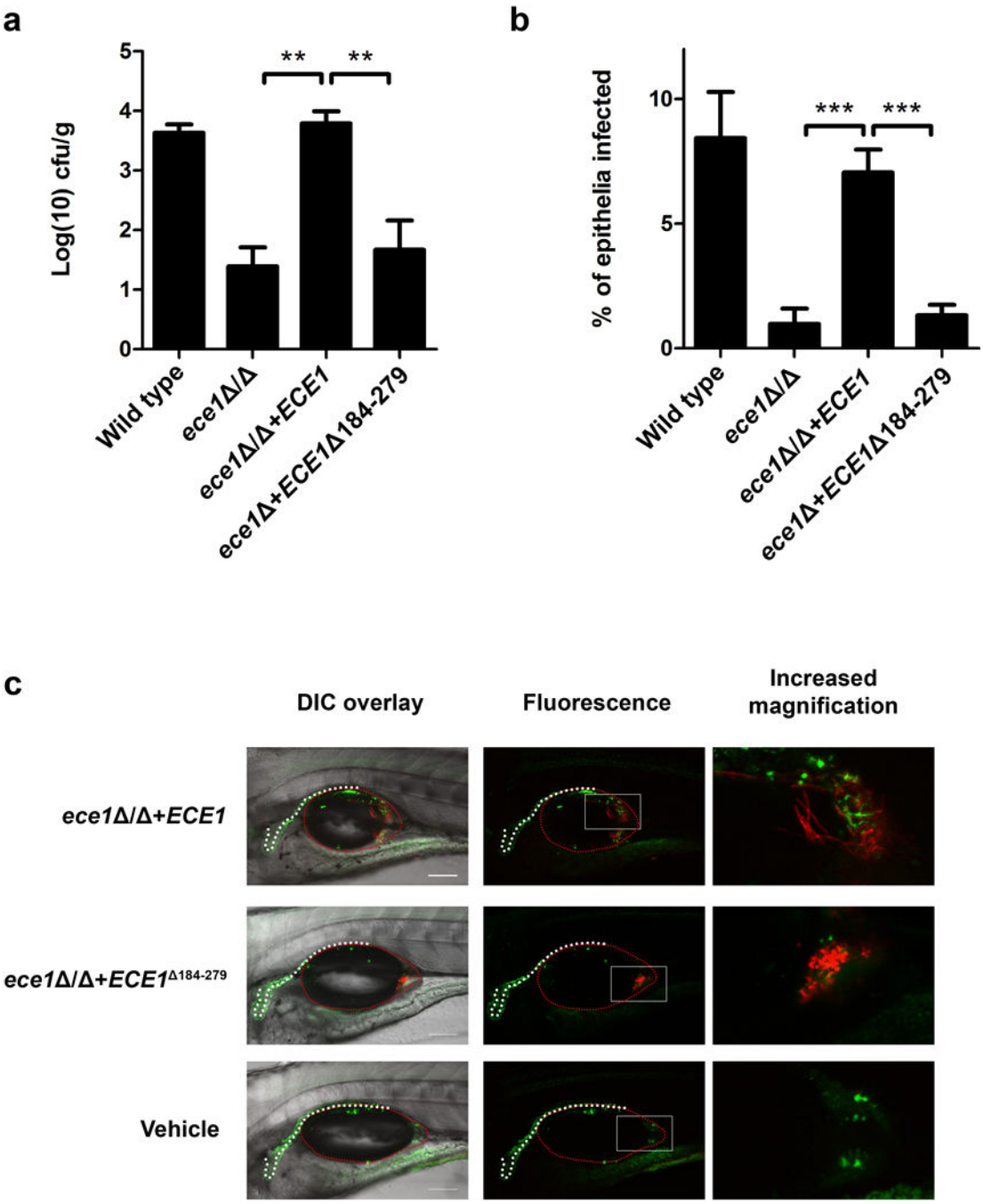

Extended Data Figure 4. Ece1-III$_{62–93}$ is required for *C. albicans* mucosal infection

(a) Fungal burdens recovered from the tongues of mice infected with *C. albicans* wild type (BWP17+CIp30) (n (number of mice) = 13), *ECE1*-deletion (*ece1Δ/Δ*) (n = 20), *ECE1* re-integrant (*ece1Δ/Δ+ECE1*) (n = 24) and Ece1-III$_{62–93}$ deletion (*ece1Δ/Δ+ECE1*$_{Δ184–279}$) (n = 10) strains after 2 day oropharyngeal infection. **(b)** Average percentage of the entire tongue epithelium area infected in different groups of mice infected with the different *C. albicans* strains. **(c)** Confocal imaging of 4 dpf zebrafish swimbladders infected with *C. albicans* Ece1-III$_{62–93}$ deletion (*ece1Δ/Δ+ECE1*$_{Δ184–279}$*+dTomato*) and *ECE1* re-integrant

(*ece1Δ/Δ+ECE1+dTomato*) strains for 24 h stained with the fluorescent exclusion dye Sytox Green. *C. albicans* cells appear red and damaged cells appear green. White dots outline the pronephros and red dots outline the swimbladder. Images are composites of maximum projections in the red and green channels (25 slices each, approximately 100 μm depth) with (left) or without (right) a single slice in the DIC channel overlay. Scale bars (bottom right) represent 100 μm. Data shown are the mean **(a-b)** or representative **(c)** of at least three biological replicates. Error bars show ± SEM. Data were analyzed by Mann-Whitney test. ** = $P < 0.01$, *** = $P < 0.001$.

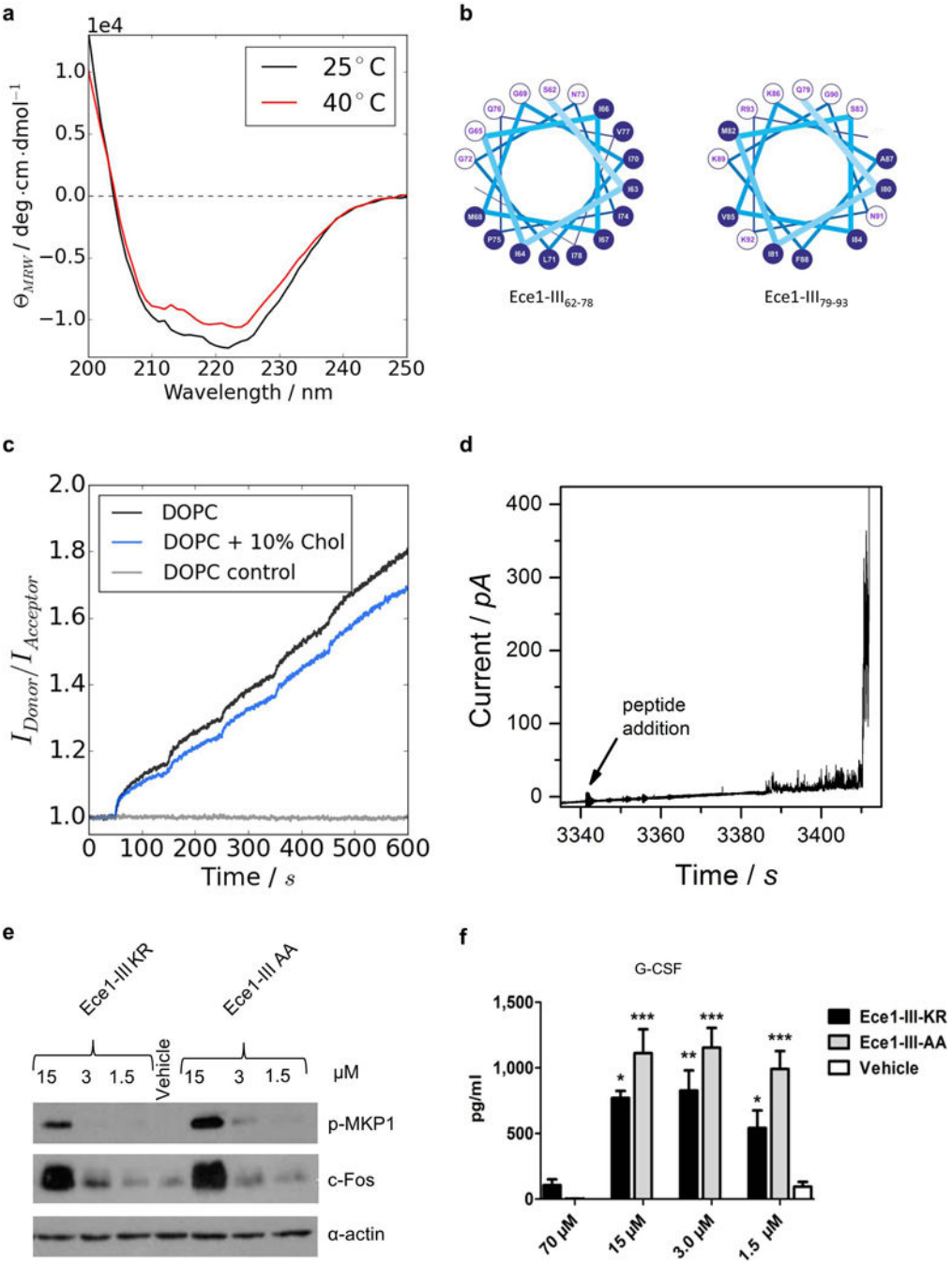

Extended Data Figure 5. Ece1-III$_{62–93}$ is a cytolytic α-helical peptide

(a) Circular dichroism spectra showing the α-helical conformation of Ece1-III$_{62–93}$ in buffer (100 mM KCl, 5 mM HEPES, pH 7). Increasing the temperature from 25°C to 40°C did not affect the stability of the α-helical structure. **(b)** Diagram to illustrate the amphipathic nature of Ece1-III$_{62–93}$ (residues 62–78, left panel; residues 79–93, right panel). Residues with hydrophobic or polar/charged side chains are displayed with a blue and white background, respectively. Modified from output generated in PEPWHEEL (http://emboss.bioinformatics.nl/cgi-bin/emboss/pepwheel). **(c)** Förster resonance energy transfer

(FRET) experiments show the intercalation of Ece1-III$_{62–93}$ into lipid liposomes (10 μM) composed of DOPC in the absence or presence of cholesterol. Peptide titration of Ece1-III$_{62–93}$ to liposomes showed slightly enhanced intercalation for pure DOPC. **(d)** Ece1-III$_{62–93}$ induced the permeabilization of planar lipid membranes composed of DOPC. The graph shows heterogeneous and transient lesions leading finally to a rupture of the membrane. Ece1-III$_{62–93}$ concentration was 0.125 μM. **(e)** Induction of p-MKP-1 and c-Fos 2 h in TR146 cells post stimulation (p.s.) with Ece1-III$_{62–93KR}$ or Ece1-III$_{62–93AA}$**(f)** Secretion of G-CSF from TR146 cells 24 h p.s. with Ece1-III$_{62–93KR}$ or Ece1-III$_{62–93AA}$. Data shown are representative (**a-e**) or mean (**f**) of at least three biological replicates. Error bars show ± SEM. Data were analyzed by one-way ANOVA (**f**). * = $P < 0.05$, ** = $P < 0.01$, *** = $P < 0.001$ (compared with vehicle control). For gel source data, see Supplementary Figure 1.

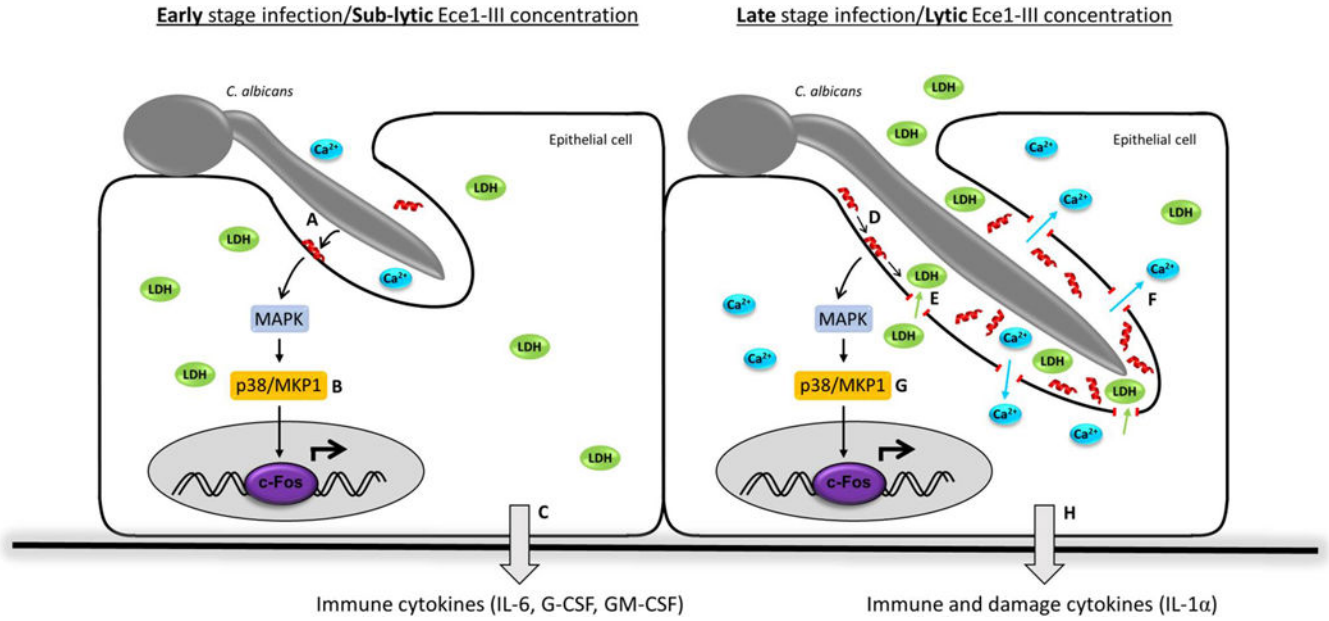

Extended Data Figure 6. Schematic of the role of Ece1-III in *C. albicans* infection of epithelial cells

During early stage infection of the mucosal surface by *C. albicans*, Ece1-III (red α-helix) is secreted into the invasion pocket created by the invading hypha **(a)**. Sub-lytic concentrations of Ece1-III trigger epithelial signal transduction through MAPK, p38/MKP-1 and c-Fos **(b)** resulting in the production of immune regulatory cytokines **(c)**. As the severity of the infection increases, Ece1-III accumulates **(d)** and once lytic concentrations are reached, causes membrane damage and the release of lactate dehydrogenase from the host epithelium **(e)**, concomitant with calcium influx **(f)**. Epithelial signal transduction is maintained **(g)** and additionally induces the release of damage associated cytokines, such as IL-1α **(h)**. Ece1-III may also have activity on the epithelial surface outside of the invasion pocket and on neighboring cells not in contact with hyphae if Ece1-III is produced in sufficient concentrations.

Extended Data Table 1

C. albicans strains used in this study.

Strain name	Strain/Gene Function	Strain Reference	Morphology*	Phospho MKP1†	c-Fos†	Cytokines‡	Damage§	Phenotype Reference
Controls								
SC5314	Wild type	[52]	Hyphae	Yes	Yes	Yes	Yes	This study
BWP17 & CIp30	Parental strain	[53]	Hyphae	Yes	Yes	Yes	Yes	This study
CAI-4 & CIp10	Parental strain	[54]	Hyphae	Yes	Yes	Yes	Yes	This study
CAF2-1	Parental strain	[54]	Hyphae	Yes	Yes	Yes	Yes	This study
DAY286	Parental strain	[55]	Hyphae	Yes	Yes	Yes	Yes	This study
Yeast-locked								
efg1Δ/Δ	*Transcription factor*	[56]	Yeast	No	No	No	No	This study
efg1/cph1Δ/Δ	*Transcription factor/ Transcription factor*	[57]	Yeast	No	No	No	No	[58]/This study
eed1Δ/Δ	*RNA polymerase II regulator*	[59]	Yeast	No	No	No	No	[58]/This study
flo8Δ/Δ	*Transcription factor*	[60]	Yeast	No	No	No	No	This study
tpk1Δ/Δ	*cAMP-dependent protein kinase*	[61]	Yeast	No	No	No	No	This study
tpk2Δ/Δ	*cAMP-dependent protein kinase*	[62]	Yeast	No	No	No	No	This study
vps11Δ/Δ	*Protein trafficking*	[63]	Yeast	No	No	No	No	This study
cap1Δ/Δ	*Transcription factor*	[64]	Yeast	No	No	Yes	No	This study
och1Δ/Δ	Alpha-1,6-mannosyltransferase	[65]	Yeast	No	No	No	No	[66]
kex2Δ/Δ	Processing enzyme	[67]	Yeast	No	No	No	No	This study
Hypha-producing								
nrg1Δ/Δ	Transcriptional corepressor	[68]	Hyphae	Yes	Yes	Yes	Yes	[58]/This study
cph1Δ/Δ	*Transcription factor*	[69]	Hyphae	Yes	Yes	Yes	Yes	This study
cph2Δ/Δ	*Transcription factor*	[70]	Hyphae	Yes	Yes	Yes	Yes	This study
efh1Δ/Δ	*Transcription factor*	[71]	Hyphae	Yes	Yes	Yes	Yes	This study
czf1Δ/Δ	*Transcription factor*	[72]	Hyphae	Yes	Yes	Yes	Yes	This study
rfg1Δ/Δ	Transcriptional repressor	[73]	Hyphae	Yes	Yes	Yes	Yes	This study
hog1Δ/Δ	*MAP kinase*	[74]	Hyphae	Yes	Yes	Yes	Yes	This study
sun42Δ/Δ	*Adhesin-like protein*	[75]	Hyphae	Yes	Yes	Yes	Yes	This study
pga29Δ/Δ	*GPI-anchored yeast-associated protein*	[76]	Hyphae	Yes	Yes	Yes	Yes	This study
phr2Δ/Δ	*Glycosidase*	[77]	Hyphae	Yes	Yes	Yes	Yes	This study
pga36Δ/Δ	*GPI-anchored protein*	[78]	Hyphae	Yes	Yes	Yes	Yes	This study
ece1Δ/Δ	*Hypha-associated protein*	[79] //	Hyphae	No	No	No	No	This study
mkc1Δ/Δ	*MAP kinase*	[80]	Hyphae	Yes	Yes	Yes	Yes	This study
bud2Δ/Δ	*GTPase activating protein*	[81]	Hyphae	Yes	Yes	Yes	Yes	This study
pra1Δ/Δ	*Zinc binding protein*	[82]	Hyphae	Yes	Yes	Yes	Yes	This study
utr2/crh11/crh12Δ/Δ	*Putative wall glycosidase/transglycosylase*	[83]	Hyphae	Yes	Yes	Yes	Yes	This study
wap1Δ/Δ	*Surface antigen on hyphae/buds*	[84]	Hyphae	Yes	Yes	Yes	Yes	This study
sod5Δ/Δ	*Superoxide dismutase*	[85]	Hyphae	Yes	Yes	Yes	Yes	This study
hwp1Δ/Δ	*Adhesin*	[86]	Hyphae	Yes	Yes	Yes	Yes	This study
rbt1Δ/Δ	*Putative GPI-modified cell wall protein*	[84]	Hyphae	Yes	Yes	Yes	Yes	This study
rbt5Δ/Δ	*Heme binding*	[84]	Hyphae	Yes	Yes	Yes	Yes	This study
hyr1Δ/Δ	*GPI-anchored hyphal cell wall protein*	[87]	Hyphae	Yes	Yes	Yes	Yes	This study
mp65Δ/Δ	*Cell surface mannoprotein*	[88]	Hyphae	Yes	Yes	yes	Yes	This study
cek1Δ/Δ	*ERK-family protein kinase*	[89]	Hyphae	Yes	Yes	Yes	Yes	This study
sap2Δ/Δ	*Secreted aspartyl protease*	[90]	Hyphae	Yes	Yes	Yes	Yes	This study
sap7Δ/Δ	*Secreted aspartyl protease*	[91]	Hyphae	Yes	Yes	Yes	Yes	This study
sap9/sap10Δ/Δ	*Secreted aspartyl proteases*	[92]	Hyphae	Yes	Yes	Yes	Yes	This study
als1Δ/Δ	*Agglutinin-like sequence protein*	[93]	Hyphae	Yes	Yes	Yes	Yes	[94]
als2Δ/ PMAL-ALS2	*Agglutinin-like sequence protein*	[95]	Hyphae	Yes	Yes	Yes	Yes	[94]
als3Δ/Δ	*Adhesin*	[93]	Hyphae	Yes	Yes	Partial//	Partial//	[94]
als4Δ/Δ	*Agglutinin-like sequence protein*	[95]	Hyphae	Yes	Yes	Yes	Yes	[94]

Strain name	Strain/Gene Function	Strain Reference	Morphology*	Phospho MKP1†	c-Fos†	Cytokines‡	Damage§	Phenotype Reference
als5Δ/Δ	*Agglutinin-like sequence protein*	[96]	Hyphae	Yes	Yes	Yes	Yes	[94]
als6Δ/Δ	*Agglutinin-like sequence protein*	[96]	Hyphae	Yes	Yes	Yes	Yes	[94]
als7Δ/Δ	*Agglutinin-like sequence protein*	[96]	Hyphae	Yes	Yes	Yes	Yes	[94]
als9Δ/Δ	*Agglutinin-like sequence protein*	[97]	Hyphae	Yes	Yes	Yes	Yes	[94]
pmt1Δ/Δ	*Mannosyltransferase*	[98]	Hyphae	Partial¶	Partial¶	Partial¶	Partial¶	[66]
pmr1Δ/Δ	*Secretory pathway ATPase*	[99]	Hyphae	Partial¶	Partial¶	Partial¶	Partial¶	[66]
mnn4Δ/Δ	Regulator of mannosylphosphorylation	[100]	Hyphae	Yes	Yes	Yes	Yes	[66]
mnn9Δ/Δ	Putative mannosyltransferase	[101]	Hyphae	Yes	Yes	Yes	Yes	[66]
mnt1/mnt2Δ/Δ	Mannosyltransferases	[102]	Hyphae	Yes	Yes	Yes	Yes	[66]
chs2/chs3Δ/Δ	Chitin synthase/ Chitin synthase	[103]	Hyphae	Yes	Yes	Yes	Yes	This study
mit1Δ/Δ	Mannose:Inositolphosphoceramide mannose transferase	[104]	Hyphae	Yes	Yes	Yes	Yes	[66]
bmt1Δ/Δ	Beta-mannosyltransferase	[105]	Hyphae	Yes	Yes	Yes	Yes	[66]
bmt2Δ/Δ	Putative beta-mannosyltransferase	[105]	Hyphae	Yes	Yes	Yes	Yes	[66]
bmt3Δ/Δ	Beta-mannosyltransferase	[105]	Hyphae	Yes	Yes	Yes	Yes	[66]
bmt4Δ/Δ	Beta-mannosyltransferase	[105]	Hyphae	Yes	Yes	Yes	Yes	[66]
bmt5Δ/Δ	Putative beta-mannosyltransferase	[106]	Hyphae	Yes	Yes	Yes	Yes	[66]
bmt6Δ/Δ	Beta-mannosyltransferase	[106]	Hyphae	Yes	Yes	Yes	Yes	[66]
gsc1Δ/GSC1	Beta-1,3-glucan synthase catalytic subunit	[107]	Hyphae	Yes	Yes	Yes	Yes	[66]
gsl1Δ/Δ	Beta-1,3-glucan synthase subunit	[107]	Hyphae	Yes	Yes	Yes	Yes	[66]
gsl2Δ/Δ	Beta-1,3-glucan synthase subunit	[107]	Hyphae	Yes	Yes	Yes	Yes	[66]
kre6Δ/KRE6	Beta-1,6-glucan synthase subunit	[108]	Hyphae	Yes	Yes	Yes	Yes	This study

*Morphology recorded 2 h post-infection on TR146 buccal epithelial cell monolayers; hyphae includes pseudohyphae.

†Data based on Western blotting.

‡Cytokines includes IL-1α, IL-6 and G-CSF.

§Damage measured by LDH assay.

¶New *ece1Δ/Δ* also created in this study (See Extended Data Table 2). Original mutant (in red) produced by [27] using the URA-blaster protocol [3]. A set of *ece1* mutants, including partial deletion of *ECE1* and a revertant, was produced in this study in the same genetic background using strain BWP17 to avoid a URA3 effect based on genomic location [109110].

¶Partial activation is due to lack of adhesion.

Extended Data Table 2

C. *albicans* mutant strains constructed and used in this study.

Strain description	Strain name	Genotype
BWP17+Clp30	M1477	*ura3: :λim m434/ura3: :λ imm434 iro1::λimm434/iro1::λimm434 his1 ::hisG/his1 ::hisG arg4: :hisG/arg4: :hisG RPS1/rps1::(URA3-HIS1-ARG4)*
ece1 Δ/Δ	M2057	*ura3: :λim m434/ura3: :λ imm434 iro1 ::Aimm434/iro1 ::λimm434 his1::hisG/his1::hisG arg4::hisG/arg4::hisG ece1::HIS1/ece1::ARG4 RPS1/rps1::URA3*
ece1Δ/Δ+ECE1	M2059	*ura3: :λim m434/ura3: :λimm434 iro1 ::λimm434/iro1 ::λimm434 his1::hisG/his1: :hisG arg4: :hisG/arg4: :hisG ece1 ::HIS1/ece1 ::ARG4 RPS1/rps1 ::(URA3-ECE1)*
ece1Δ/Δ+ECE1$_{\Delta 184\_279}$	M2174	*ura3: :λim m434/ura3: :λimm434 iro1 :λimm434/iro1 ::λimm434 his1::hisG/his1::hisG*

Strain description	Strain name	Genotype
		arg4: :hisG/arg4: :hisG ece1::HIS1/ece1::ARG4 RPS1/rps1 ::(URA3-ECE1$^{\Delta 184–279}$)
*K*ex1Δ/Δ	M2258	*ura3: :λim m434/uro3: :λimm434 iro1 ::λimm434/iro1 ::λimm434 his1::hisG/his1: :hisG arg4::hisG/arg4: :hisG kex1::HIS1/kex1::ARG4 RPS1/rps1::URA3*
SC5314+pECE1-GFP (ECE1 promoter-GFP)	CA58	*ECE1/ece1::GFP-SAT1*
BWP17+Clp30+*pENO1-dTom (ENO1* promoter-dTom)	RWC83	*ura3::λimm434/ura3::λimm434 iro1 ::λimm434/iro1 ::λimm434 his1 ::hisG/his1 ::hisG arg4: :hisG/arg4: :hisG RPS1rps1 ::(URA3-HIS1-ARG4) EN01/eno1::dTom-SAT1*
ece1Δ/Δ+*pENO1*-dTom (*ENO1* promoter-dTom)	RWC84	*ura3: :λim m434/ura3: :λimm434 iro1 ::λimm434/iro1 ::λimm434 his1::hisG/his1: :hisG arg4: :hisG/arg4: :hisG ece1 ::HIS1/ece1 ::ARG4 RPS1/rps1::URA3 EN01/enol::dTom-SAT1*
ece1Δ/Δ+ECE1+ dTomato	RWC85	*ura3: :λim m434/ura3: :λimm434 iro1: :λimm 43 4/iro1: :λim m434 his1::hisG/his1::hisG arg4: :hisG/arg4: :hisG ece1 ::HIS1/ece1 ::ARG4 RPS1/rps1::(URA3-ECE1) EN01/eno1::dTomato-NAT*
ece1Δ/Δ+ECE1$_{\Delta 184–279}$ + dTomato	RWC86	*ura3::λimm434/ura3::λimm434 iro1 ::λimm434/iro1 ::λimm434 his1::hisG/his1: :hisG arg4: :hisG/arg4: :hisG ece1 ::HIS1/ece1 ::ARG4 RPS1/rps1 ::(URA3-ECE1$^{\Delta 184–279}$) EN01/eno1::dTomato-NAT*

Extended Data Table 3

LC-MS/MS analysis of *C. albicans* Ece1-III

Ece1-III sequence	PSM Value* (% total Ece1-III†) (% total Ece1p‡)				
	Wild Type	*ece1Δ/Δ+ECE1*	TR146+Wild type	rEce1p+rKex2p	*kex1Δ/Δ*
SIIGIIMGILGNIPQVIQIIMSIVKAFKGNK	699 (86%) (41%)	477 (89%) (35%)	79 (97.5%) (97.5%)	n/d§	49 (13.3%) (3.6%)
SIIGIIMGILGNIPQVIQIIMSIVKAFKGNKR	1 (0.1%) (0.06%)	1 (0.2%) (0.07%)	2 (2.5%) (2.5%)	248 (80%) (1.5%)	291 (78.9%) (21%)

*The number of peptide spectrum matches. Data for *ece1Δ/Δ* and *ece1Δ/Δ+ECE1Δ184–279* are not included as no Ece1-III peptides were detected in either strain, as expected.

†% of SIIGIIMGILGNIPQVIQIIMSIVKAFKGNK or SIIGIIMGILGNIPQVIQIIMSIVKAFKGNKR detected amongst all Ece1-III peptides found by LC-MS/MS.

‡% of SIIGIIMGILGNIPQVIQIIMSIVKAFKGNK or SIIGIIMGILGNIPQVIQIIMSIVKAFKGNKR detected amongst all Ecelp peptides found by LC-MS/MS.

§n/d; not detected.

Extended Data Table 4

Oligonucleotide primers used in this study.

Primer name	Application	Sequence (5′-3′)	Description
ECE1-FG	PCR	atcaaataacccacctatttcaaaattgttttatttttgtttatctctacaaca aacaactttccttttattttactaccaactattttccattcgttaaagaagcttc gtacgctgcaggtc	Construction of *ECE1* deletion construct
ECE1-RG	PCR	cacaaaaaacaacaattaaaaaaatcagttacagcaaaagtgtcacaag acttatggaataaaagattaagcttgtggaaaacaaatttttatctgctgag cattctgatatcatcgatgaattcgag	Construction of *ECE1* deletion construct
ECE1-RecF3k	PCR	gcacgcgtctaaagtggagtaacaac	Construction of *ECE1* complementation plasmid
ECE1-RecR	PCR	ggtcgaccccagacgttggttgc	Construction of *ECE1* complementation plasmid
ECE1-F1	PCR	ggcttctcataaatgaagggctcag	Confirmation of *ECE1* deletion
ECE1-R1	PCR	gccgaatcaatcttgtcgtgccac	Confirmation of *ECE1* deletion
KEX1-FG	PCR	tatctttttttgttttatttacccatccttcatatctttacaacccttgatacctt acctaaacaacacacatctatctttaatcaatcaaacacaaatcaattgaa gcttcgtacgctgcaggtc	Construction of *KEX1* deletion construct
KEX1-RG	PCR	tcacaatctagattattgtaggttgtatagacaaaaaataaaaatcaaact attattcgttatataaatctacaagatctctaatctccactgtaccgaaaaat tctgatatcatcgatgaattcgag	Construction of *KEX1* deletion construct
KEX1-F1	PCR	ggaagcccataagaaattgga	Confirmation of *KEX1* deletion
KEX1-R1	PCR	aggaagctgtggtggtagtg	Confirmation of *KEX1* deletion
HIS-F2	PCR	ggacgaattgaagaaagctggtgcaaccg	Confirmation of *ECE1/KEX1* deletion
HIS-R2	PCR	caacgaaatggcctcccctaccacag	Confirmation of *ECE1/KEX1* deletion
ARG-F2	PCR	ggatatgttggctactgatttag	Confirmation of *ECE1/KEX1* deletion
ARG-R2	PCR	aatggatcagtggcaccggtg	Confirmation of *ECE1/KEX1* deletion
ECE1-Flnt1	PCR	ctaacgtttttgatggcgtcctgg	Confirmation of plasmid integration
URAF2	PCR	ggagttggattagatgataaaggtgatgg	Confirmation of plasmid integration
RPF-1	PCR	gagcagtgtacacacacacatcttg	Confirmation of plasmid integration
RPF-2	PCR	cgccaaagagtttcccctattatc	Confirmation of plasmid integration
Pep3-F1	PCR	gaagatatcgattctgttgttgctgg	Excision of Ece1-lll$_{62–93}$ from *ECE1*
Pep3-R1	PCR	cagaatcgatatcttctcttttggtaatagcagtattgaattcttg	Excision of Ece1-lll$_{62–93}$ from *ECE1*
5′ECE1prom-Nar1	PCR	gatcggcgcctccagccactattttgtacctgt	Amplification of *ECE1* promoter region for *ECE1* promoter-GFP construct
3′ECE1prom-Xhol	PCR	tcagctcgagtttaacgaatggaaaatagttggtag	Amplification of *ECE1* promoter region for *ECE1* promoter-GFP construct
5′ECE1term-SacII	PCR	gatcccgcggcagcagataaaaatttgttttccacaag	Amplification of *ECE1* terminator region for

Primer name	Application	Sequence (5′-3′)	Description
			ECE1 promoter-GFP construct
5′ECE1term-SacI	PCR	tcaggagctccgttaagaatatgaatgacagttggtc	Amplification of *ECE1* terminator region for *ECE1* promoter-GFP construct
G1-ECE1	PCR	ctcgctgattagagttcaagagt	Confirmation of *ECE1*-GFP plasmid integration (5′ end)
GFP veri rev	PCR	tgatctgggtatctcgcaaagcat	Confirmation of *ECE1*-GFP plasmid integration (5′ end)
G4-ECE1	PCR	tggaagattcacttgagttggaac	Confirmation of *ECE1-GFP* plasmid integration (3′ end)
X3-SAT1	PCR	gtgaagtgtgaaggggag	Confirmation of *ECE1-GFP* plasmid integration (3′ end)
pENO1FW	PCR	tccttggctggca ctga a ctcg	Confirmation of pENO1-dTom plasmid integration
dTom REV	PCR	aaggtctaccttcaccttcacc	Confirmation of pENO1-dTom plasmid integration
ACT1-F	qPCR	tcagaccagctgatttaggtttg	Quantification of actin cDNA
ACT1-R	qPCR	gtgaacaatggatggaccag	Quantification of actin cDNA
ECE1-F	qPCR	atcgaaaatgccaagagag	Quantification of *ECE1* cDNA
ECE1-R	qPCR	agcattttcaataccgacag	Quantification of *ECE1* cDNA

Supplementary Material

Refer to Web version on PubMed Central for supplementary material.

Acknowledgments

We thank Sarah Gaffen, Bruce Klein, Christian Hertweck, Abigail Tucker, Jeremy Green and Stephen Challacombe for comments on the manuscript. For experimental assistance we thank Stuart Bevan and David Andersson (calcium assays), Deepa Nayar (histology), Durdana Rahman and Mukesh Mistry (murine model), Mark Nilan (zebrafish model), Sabrina Groth (FRET spectroscopy), Nadine Gebauer (Impedance experiments), Daniela Schulz (*kex1*Δ/Δ strain) and our colleagues for supplying fungal mutant strains. This work was supported by grants from the Medical Research Council (MR/J008303/1, MR/M011372/1), Biotechnology & Biological Sciences Research Council (BB/J015261/1), FP7-PEOPLE-2013-Initial Training Network (606786) to JRN; Wellcome Trust Strategic Award for Medical Mycology and Fungal Immunology (097377/Z/11/Z) to JRN and DW; Sir Henry Dale Fellowship jointly funded by the Wellcome Trust and the Royal Society (102549/Z/13/Z) to DW; Deutsche Forschungsgemeinschaft CRC/TR124 FungiNet Project C1 and Z2, Deutsche Forschungsgemeinschaft SPP 1580 (Hu 528/17-1) and CSCC, German Federal Ministry of Education and Health [BMBF] 01EO1002 to BHu; Cluster of Excellence ‘Inflammation at interfaces’ and Deutsche Forschungsgemeinschaft SPP1580 project GU 568/5-1 to TG; National Institutes of Health (R15AI094406) and the Burroughs Wellcome Fund to RTW.

References

1. Brown GD, et al. Hidden killers: human fungal infections. Sci Transl Med. 2012; 4 165rv113.
2. Jacobsen ID, et al. *Candida albicans* dimorphism as a therapeutic target. Expert Rev Anti Infect Ther. 2012; 10:85–93. [PubMed: 22149617]
3. Moyes DL, et al. A Biphasic Innate Immune MAPK Response Discriminates between the Yeast and Hyphal Forms of *Candida albicans* in Epithelial Cells. Cell Host Microbe. 2010; 8:225–235. [PubMed: 20833374]

4. Moyes DL, et al. Candida albicans yeast and hyphae are discriminated by MAPK signaling in vaginal epithelial cells. PLoS ONE. 2011; 6:e26580. [PubMed: 22087232]
5. Murciano C, et al. *Candida albicans* cell wall glycosylation may be indirectly required for activation of epithelial cell proinflammatory responses. Infect Immun. 2011; 79:4902–4911. [PubMed: 21930756]
6. Moyes DL, et al. Activation of MAPK/c-Fos induced responses in oral epithelial cells is specific to *Candida albicans* and *Candida dubliniensis* hyphae. Med Microbiol Immunol. 2012; 201:93–101. [PubMed: 21706283]
7. Murciano C, et al. Evaluation of the role of *Candida albicans* agglutinin-like sequence (Als) proteins in human oral epithelial cell interactions. PLoS ONE. 2012; 7:e33362. [PubMed: 22428031]
8. Moyes DL, Naglik JR. Mucosal Immunity and *Candida albicans* Infection. Clin Dev Immunol. 2011; 2011
9. Naglik JR, Moyes D. Epithelial Cell Innate Response to *Candida albicans* . Adv Dent Res. 2011; 23:50–55. [PubMed: 21441481]
10. Naglik JR, Moyes DL, Wachtler B, Hube B. *Candida albicans* interactions with epithelial cells and mucosal immunity. Microbes Infect. 2011; 13:963–976. [PubMed: 21801848]
11. Hebecker B, Naglik JR, Hube B, Jacobsen ID. Pathogenicity mechanisms and host response during oral *Candida albicans* infections. Expert Rev Anti Infect Ther. 2014; 12:867–879. [PubMed: 24803204]
12. Naglik JR. *Candida* Immunity. New Journal of Science. 2014; 2014 Article ID 390241, 390227 pages.
13. Naglik JR, Richardson JP, Moyes DL. *Candida albicans* Pathogenicity and Epithelial Immunity. PLoS Pathog. 2014; 10:e1004257. [PubMed: 25121985]
14. Moyes DL, Richardson JP, Naglik JR. *Candida albicans*-epithelial interactions and pathogenicity mechanisms: scratching the surface. Virulence. 2015; 6:338–346. [PubMed: 25714110]
15. Birse CE, Irwin MY, Fonzi WA, Sypherd PS. Cloning and characterization of *ECE1*, a gene expressed in association with cell elongation of the dimorphic pathogen *Candida albicans* . Infect Immun. 1993; 61:3648–3655. [PubMed: 8359888]
16. Rohm M, et al. A family of secreted pathogenesis-related proteins in *Candida albicans* . Mol Microbiol. 2013; 87:132–151. [PubMed: 23136884]
17. Kamai Y, Kubota M, Hosokawa T, Fukuoka T, Filler SG. New model of oropharyngeal candidiasis in mice. Antimicrob Agents Chemother. 2001; 45:3195–3197. [PubMed: 11600377]
18. Brothers KM, et al. NADPH Oxidase-Driven Phagocyte Recruitment Controls *Candida albicans* Filamentous Growth and Prevents Mortality. PLoS Pathog. 2013; 9:e1003634. [PubMed: 24098114]
19. Gratacap RL, Rawls JF, Wheeler RT. Mucosal candidiasis elicits NF-kappaB activation, proinflammatory gene expression and localized neutrophilia in zebrafish. Dis Model Mech. 2013; 6:1260–1270. [PubMed: 23720235]
20. Bader O, Krauke Y, Hube B. Processing of predicted substrates of fungal Kex2 proteinases from *Candida albicans, C. glabrata, Saccharomyces cerevisiae* and *Pichia pastoris* . BMC Microbiol. 2008; 8:116. [PubMed: 18625069]
21. Newport G, Agabian N. *KEX2* influences *Candida albicans* proteinase secretion and hyphal formation. J Biol Chem. 1997; 272:28954–28961. [PubMed: 9360967]
22. Liu P, Huang X, Zhou R, Berne BJ. Observation of a dewetting transition in the collapse of the melittin tetramer. Nature. 2005; 437:159–162. [PubMed: 16136146]
23. Bechinger B, Salnikov ES. The membrane interactions of antimicrobial peptides revealed by solid-state NMR spectroscopy. Chem Phys Lipids. 2012; 165:282–301. [PubMed: 22366307]
24. Pieta P, Mirza J, Lipkowski J. Direct visualization of the alamethicin pore formed in a planar phospholipid matrix. Proc Natl Acad Sci U S A. 2012; 109:21223–21227. [PubMed: 23236158]
25. Bischofberger M, Iacovache I, van der Goot FG. Pathogenic pore-forming proteins: function and host response. Cell Host Microbe. 2012; 12:266–275. [PubMed: 22980324]
26. Los FC, Randis TM, Aroian RV, Ratner AJ. Role of pore-forming toxins in bacterial infectious diseases. Microbiol Mol Biol Rev. 2013; 77:173–207. [PubMed: 23699254]

27. Oren Z, Shai Y. Selective lysis of bacteria but not mammalian cells by diastereomers of melittin: structure-function study. Biochem. 1997; 36:1826–1835. [PubMed: 9048567]
28. Walev I, et al. Delivery of proteins into living cells by reversible membrane permeabilization with streptolysin-O. Proc Natl Acad Sci U S A. 2001; 98:3185–3190. [PubMed: 11248053]
29. Schmitt MJ, Breinig F. Yeast viral killer toxins: lethality and self-protection. Nat Rev Microbiol. 2006; 4:212–221. [PubMed: 16489348]
30. Zakikhany K, et al. In vivo transcript profiling of *Candida albicans* identifies a gene essential for interepithelial dissemination. Cell Microbiol. 2007; 9:2938–2954. [PubMed: 17645752]
31. Wachtler B, et al. *Candida albicans*-epithelial interactions: dissecting the roles of active penetration, induced endocytosis and host factors on the infection process. PLoS ONE. 2012; 7:e36952. [PubMed: 22606314]
32. Rupniak HT, et al. Characteristics of four new human cell lines derived from squamous cell carcinomas of the head and neck. J Natl Cancer Inst. 1985; 75:621–635. [PubMed: 2413234]
33. Mayer FL, et al. The novel *Candida albicans* transporter Dur31 Is a multi-stage pathogenicity factor. PLoS pathog. 2012; 8:e1002592. [PubMed: 22438810]
34. Gillum AM, Tsay EY, Kirsch DR. Isolation of the *Candida albicans* gene for orotidine-5′-phosphate decarboxylase by complementation of S. cerevisiae ura3 and *E. coli* pyrF mutations. Mol Gen Genet. 1984; 198:179–182. [PubMed: 6394964]
35. Citiulo F, et al. Candida albicans scavenges host zinc via Pra1 during endothelial invasion. PLoS pathog. 2012; 8:e1002777. [PubMed: 22761575]
36. Gola S, Martin R, Walther A, Dunkler A, Wendland J. New modules for PCR-based gene targeting in *Candida albicans*: rapid and efficient gene targeting using 100 bp of flanking homology region. Yeast. 2003; 20:1339–1347. [PubMed: 14663826]
37. Wilson RB, Davis D, Mitchell AP. Rapid hypothesis testing with *Candida albicans* through gene disruption with short homology regions. J Bacteriol. 1999; 181:1868–1874. [PubMed: 10074081]
38. Walther A, Wendland J. An improved transformation protocol for the human fungal pathogen *Candida albicans* . Curr Genet. 2003; 42:339–343. [PubMed: 12612807]
39. Murad AM, Lee PR, Broadbent ID, Barelle CJ, Brown AJ. CIp10, an efficient and convenient integrating vector for *Candida albicans* . Yeast. 2000; 16:325–327. [PubMed: 10669870]
40. Gratacap RL, Rawls JF, Wheeler RT. Mucosal candidiasis elicits NF-kappaB activation, proinflammatory gene expression and localized neutrophilia in zebrafish. Dis Model Mech. 2013; 6:1260–1270. [PubMed: 23720235]
41. Moyes DL, et al. A biphasic innate immune MAPK response discriminates between the yeast and hyphal forms of *Candida albicans* in epithelial cells. Cell Host Microbe. 2010; 8:225–235. [PubMed: 20833374]
42. Moyes DL, et al. *Candida albicans* yeast and hyphae are discriminated by MAPK signaling in vaginal epithelial cells. PloS ONE. 2011; 6:e26580. [PubMed: 22087232]
43. Wachtler B, Wilson D, Haedicke K, Dalle F, Hube B. From attachment to damage: defined genes of *Candida albicans* mediate adhesion, invasion and damage during interaction with oral epithelial cells. PloS ONE. 2011; 6:e17046. [PubMed: 21407800]
44. Trinh le A, et al. A versatile gene trap to visualize and interrogate the function of the vertebrate proteome. Gene Devel. 2011; 25:2306–2320. [PubMed: 22056673]
45. Solis NV, Filler SG. Mouse model of oropharyngeal candidiasis. Nat Protoc. 2012; 7:637–642. [PubMed: 22402633]
46. Cranfield C, Carne S, Martinac B, Cornell B. The assembly and use of tethered bilayer lipid membranes (tBLMs). Methods Mol Biol. 2015; 1232:45–53. [PubMed: 25331126]
47. Cranfield CG, et al. Transient potential gradients and impedance measures of tethered bilayer lipid membranes: pore-forming peptide insertion and the effect of electroporation. Biophys J. 2014; 106:182–189. [PubMed: 24411250]
48. Schromm AB, et al. Lipopolysaccharide-binding protein mediates CD14-independent intercalation of lipopolysaccharide into phospholipid membranes. FEBS Lett. 1996; 399:267–271. [PubMed: 8985160]

49. Chen GC, Yang JT. 2-Point Calibration of Circular Dichrometer with D-10-Camphorsulfonic Acid. Anal. Lett. 1977; 10:1195–1207.

50. Montal M, Mueller P. Formation of bimolecular membranes from lipid monolayers and a study of their electrical properties. Proc Natl Acad Sci U S A. 1972; 69:3561–3566. [PubMed: 4509315]

51. Gutsmann T, Heimburg T, Keyser U, Mahendran KR, Winterhalter M. Protein reconstitution into freestanding planar lipid membranes for electrophysiological characterization. Nat Protoc. 2015; 10:188–198. [PubMed: 25551663]

Extended Data Table references

52. Gillum AM, Tsay EY, Kirsch DR. Isolation of the *Candida albicans* gene for orotidine-5′-phosphate decarboxylase by complementation of *S. cerevisiae* ura3, *E. coli* pyrF mutations. Mol Gen Genet. 1984; 198:179–182. [PubMed: 6394964]

53. Wilson RB, Davis D, Mitchell AP. Rapid hypothesis testing with *Candida albicans* through gene disruption with short homology regions. J Bacteriol. 1999; 181:1868–1874. [PubMed: 10074081]

54. Fonzi WA, Irwin MY. Isogenic strain construction and gene mapping in *Candida albicans* . Genetics. 1993; 134:717–728. [PubMed: 8349105]

55. Davis D, Wilson RB, Mitchell AP. *RIM101*-dependent and-independent pathways govern pH responses in *Candida albicans* . Mol Cell Biol. 2000; 20:971–978. [PubMed: 10629054]

56. Braun BR, Johnson AD. TUP1, CPH1 and EFG1 make independent contributions to filamentation in *Candida albicans* . Genetics. 2000; 155:57–67. [PubMed: 10790384]

57. Lo HJ, et al. Nonfilamentous *C. albicans* mutants are avirulent. Cell. 1997; 90:939–949. [PubMed: 9298905]

58. Moyes DL, et al. A biphasic innate immune MAPK response discriminates between the yeast and hyphal forms of *Candida albicans* in epithelial cells. Cell Host Microbe. 2010; 8:225–235. [PubMed: 20833374]

59. Zakikhany K, et al. In vivo transcript profiling of *Candida albicans* identifies a gene essential for interepithelial dissemination. Cell Microbiol. 2007; 9:2938–2954. [PubMed: 17645752]

60. Cao F, et al. The Flo8 transcription factor is essential for hyphal development and virulence in *Candida albicans* . Mol Biol Cell. 2006; 17:295–307. [PubMed: 16267276]

61. Bockmuhl DP, Krishnamurthy S, Gerads M, Sonneborn A, Ernst JF. Distinct and redundant roles of the two protein kinase A isoforms Tpk1p and Tpk2p in morphogenesis and growth of *Candida albicans* . Mol Microbiol. 2001; 42:1243–1257. [PubMed: 11886556]

62. Sonneborn A, et al. Protein kinase A encoded by TPK2 regulates dimorphism of *Candida albicans* . Mol Microbiol. 2000; 35:386–396. [PubMed: 10652099]

63. Palmer GE, Cashmore A, Sturtevant J. *Candida albicans VPS11* is required for vacuole biogenesis and germ tube formation. Eukaryot Cell. 2003; 2:411–421. [PubMed: 12796286]

64. Zou H, Fang HM, Zhu Y, Wang Y. *Candida albicans* Cyr1, Cap1 and G-actin form a sensor/effector apparatus for activating cAMP synthesis in hyphal growth. Mol Microbiol. 2010; 75:579–591. [PubMed: 19943905]

65. Bates S, et al. Outer chain N-glycans are required for cell wall integrity and virulence of *Candida albicans* . J Biol Chem. 2006; 281:90–98. [PubMed: 16263704]

66. Murciano C, et al. *Candida albicans* cell wall glycosylation may be indirectly required for activation of epithelial cell proinflammatory responses. Infect Immun. 2011; 79:4902–4911. [PubMed: 21930756]

67. Newport G, Agabian N. *KEX2* influences *Candida albicans* proteinase secretion and hyphal formation. J Biol Chem. 1997; 272:28954–28961. [PubMed: 9360967]

68. Murad AM, et al. *NRG1* represses yeast-hypha morphogenesis and hypha-specific gene expression in *Candida albicans* . EMBO J. 2001; 20:4742–4752. [PubMed: 11532938]

69. Liu H, Kohler J, Fink GR. Suppression of hyphal formation in *Candida albicans* by mutation of a *STE12* homolog. Science. 1994; 266:1723–1726. [PubMed: 7992058]

70. Lane S, Zhou S, Pan T, Dai Q, Liu H. The basic helix-loop-helix transcription factor Cph2 regulates hyphal development in *Candida albicans* partly via *TEC1* . Mol Cell Biol. 2001; 21:6418–6428. [PubMed: 11533231]
71. White SJ, et al. Self-regulation of *Candida albicans* population size during GI colonization. PLoS pathog. 2007; 3:e184. [PubMed: 18069889]
72. Brown DH Jr, Giusani AD, Chen X, Kumamoto CA. Filamentous growth of *Candida albicans* in response to physical environmental cues and its regulation by the unique *CZF1* gene. Mol Microbiol. 1999; 34:651–662. [PubMed: 10564506]
73. Kadosh D, Johnson AD. Rfg1, a protein related to the *Saccharomyces cerevisiae* hypoxic regulator Rox1, controls filamentous growth and virulence in *Candida albicans* . Mol Cell Biol. 2001; 21:2496–2505. [PubMed: 11259598]
74. San Jose C, Monge RA, Perez-Diaz R, Pla J, Nombela C. The mitogen-activated protein kinase homolog *HOG1* gene controls glycerol accumulation in the pathogenic fungus *Candida albicans* . J Bacteriol. 1996; 178:5850–5852. [PubMed: 8824643]
75. Firon A, et al. The *SUN41* and *SUN42* genes are essential for cell separation in *Candida albicans* . Mol Microbiol. 2007; 66:1256–1275. [PubMed: 18001349]
76. de Boer AD, et al. The *Candida albicans* cell wall protein Rhd3/Pga29 is abundant in the yeast form and contributes to virulence. Yeast. 2010; 27:611–624. [PubMed: 20533408]
77. Muhlschlegel FA, Fonzi WA. *PHR2* of *Candida albicans* encodes a functional homolog of the pH-regulated gene *PHR1* with an inverted pattern of pH-dependent expression. Mol Cell Biol. 1997; 17:5960–5967. [PubMed: 9315654]
78. Martin R, et al. A core filamentation response network in *Candida albicans* is restricted to eight genes. PloS ONE. 2013; 8:e58613. [PubMed: 23516516]
79. Birse CE, Irwin MY, Fonzi WA, Sypherd PS. Cloning and characterization of *ECE1*, a gene expressed in association with cell elongation of the dimorphic pathogen *Candida albicans* . Infect Immun. 1993; 61:3648–3655. [PubMed: 8359888]
80. Navarro-Garcia F, Sanchez M, Pla J, Nombela C. Functional characterization of the *MKC1* gene of *Candida albicans*, which encodes a mitogen-activated protein kinase homolog related to cell integrity. Mol Cell Biol. 1995; 15:2197–2206. [PubMed: 7891715]
81. Hausauer DL, Gerami-Nejad M, Kistler-Anderson C, Gale CA. Hyphal guidance and invasive growth in *Candida albicans* require the Ras-like GTPase Rsr1p and its GTPase-activating protein Bud2p. Eukaryot Cell. 2005; 4:1273–1286. [PubMed: 16002653]
82. Sentandreu M, Elorza MV, Sentandreu R, Fonzi WA. Cloning and characterization of *PRA1*, a gene encoding a novel pH-regulated antigen of *Candida albicans* . J Bacteriol. 1998; 180:282–289. [PubMed: 9440517]
83. Pardini G, et al. The *CRH* family coding for cell wall glycosylphosphatidylinositol proteins with a predicted transglycosidase domain affects cell wall organization and virulence of *Candida albicans* . J Biol Chem. 2006; 281:40399–40411. [PubMed: 17074760]
84. Braun BR, Head WS, Wang MX, Johnson AD. Identification and characterization of *TUP1*-regulated genes in *Candida albicans* . Genetics. 2000; 156:31–44. [PubMed: 10978273]
85. Fradin C, et al. Granulocytes govern the transcriptional response, morphology and proliferation of *Candida albicans* in human blood. Mol Microbiol. 2005; 56:397–415. [PubMed: 15813733]
86. Staab JF, Bradway SD, Fidel PL, Sundstrom P. Adhesive and mammalian transglutaminase substrate properties of *Candida albicans* Hwp1. Science. 1999; 283:1535–1538. [PubMed: 10066176]
87. Bailey DA, Feldmann PJ, Bovey M, Gow NA, Brown AJ. The *Candida albicans HYR1* gene, which is activated in response to hyphal development, belongs to a gene family encoding yeast cell wall proteins. J Bacteriol. 1996; 178:5353–5360. [PubMed: 8808922]
88. Sandini S, La Valle R, De Bernardis F, Macri C, Cassone A. The 65 kDa mannoprotein gene of *Candida albicans* encodes a putative beta-glucanase adhesin required for hyphal morphogenesis and experimental pathogenicity. Cell Microbiol. 2007; 9:1223–1238. [PubMed: 17217426]
89. Csank C, et al. Roles of the *Candida albicans* mitogen-activated protein kinase homolog, Cek1p, in hyphal development and systemic candidiasis. Infect Immun. 1998; 66:2713–2721. [PubMed: 9596738]

90. Hube B, et al. Disruption of each of the secreted aspartyl proteinase genes *SAP1, SAP2*, and *SAP3* of *Candida albicans* attenuates virulence. Infect Immun. 1997; 65:3529–3538. [PubMed: 9284116]
91. Taylor BN, et al. Induction of *SAP7* correlates with virulence in an intravenous infection model of candidiasis but not in a vaginal infection model in mice. Infect Immun. 2005; 73:7061–7063. [PubMed: 16177393]
92. Schild L, et al. Proteolytic cleavage of covalently linked cell wall proteins by *Candida albicans* Sap9 and Sap10. Eukaryot Cell. 2011; 10:98–109. [PubMed: 21097664]
93. Zhao X, et al. *ALS3* and *ALS8* represent a single locus that encodes a *Candida albicans* adhesin; functional comparisons between Als3p and Als1p. Microbiol. 2004; 150:2415–2428.
94. Murciano C, et al. Evaluation of the role of *Candida albicans* agglutinin-like sequence (Als) proteins in human oral epithelial cell interactions. PloS ONE. 2012; 7:e33362. [PubMed: 22428031]
95. Zhao X, Oh SH, Yeater KM, Hoyer LL. Analysis of the *Candida albicans* Als2p and Als4p adhesins suggests the potential for compensatory function within the Als family. Microbiol. 2005; 151:1619–1630.
96. Zhao X, Oh SH, Hoyer LL. Deletion of *ALS5 ALS6* or *ALS7* increases adhesion of *Candida albicans* to human vascular endothelial and buccal epithelial cells. Med Mycol. 2007; 45:429–434. [PubMed: 17654269]
97. Zhao X, Oh SH, Hoyer LL. Unequal contribution of *ALS9* alleles to adhesion between *Candida albicans* and human vascular endothelial cells. Microbiol. 2007; 153:2342–2350.
98. Timpel C, Strahl-Bolsinger S, Ziegelbauer K, Ernst JF. Multiple functions of Pmt1p–mediated protein O-mannosylation in the fungal pathogen *Candida albicans* . J Biol Chem. 1998; 273:20837–20846. [PubMed: 9694829]
99. Bates S, et al. Candida albicans Pmr1p, a secretory pathway P-type Ca2+/Mn2+-ATPase, is required for glycosylation and virulence. J Biol Chem. 2005; 280:23408–23415. [PubMed: 15843378]
100. Hobson RP, et al. Loss of cell wall mannosylphosphate in *Candida albicans* does not influence macrophage recognition. J Biol Chem. 2004; 279:39628–39635. [PubMed: 15271989]
101. Southard SB, Specht CA, Mishra C, Chen-Weiner J, Robbins PW. Molecular analysis of the *Candida albicans* homolog of *Saccharomyces cerevisiae MNN9*, required for glycosylation of cell wall mannoproteins. J Bacteriol. 1999; 181:7439–7448. [PubMed: 10601199]
102. Munro CA, et al. Mnt1p and Mnt2p of *Candida albicans* are partially redundant alpha-1,2-mannosyltransferases that participate in O-linked mannosylation and are required for adhesion and virulence. J Biol Chem. 2005; 280:1051–1060. [PubMed: 15519997]
103. Mio T, et al. Role of three chitin synthase genes in the growth of *Candida albicans* . J Bacteriol. 1996; 178:2416–2419. [PubMed: 8636047]
104. Mille C, et al. Inactivation of *CaMIT1* inhibits *Candida albicans* phospholipomannan beta-mannosylation, reduces virulence, and alters cell wall protein beta-mannosylation. J Biol Chem. 2004; 279:47952–47960. [PubMed: 15347680]
105. Mille C, et al. Identification of a new family of genes involved in beta-1,2-mannosylation of glycans in *Pichia pastoris* and *Candida albicans* . J Biol Chem. 2008; 283:9724–9736. [PubMed: 18234669]
106. Mille C, et al. Members 5 and 6 of the Candida albicans *BMT* family encode enzymes acting specifically on beta-mannosylation of the phospholipomannan cell-wall glycosphingolipid. Glycobiol. 2012; 22:1332–1342.
107. Mio T, et al. Cloning of the *Candida albicans* homolog of *Saccharomyces cerevisiae GSC1/FKS1* and its involvement in beta-1,3-glucan synthesis. J Bacteriol. 1997; 179:4096–4105. [PubMed: 9209021]
108. Mio T, et al. Isolation of the *Candida albicans* homologs of *Saccharomyces cerevisiae KRE6* and *SKN1*: expression and physiological function. J Bacteriol. 1997; 179:2363–2372. [PubMed: 9079924]
109. Staab JF, Sundstrom P. *URA3* as a selectable marker for disruption and virulence assessment of *Candida albicans* genes. Trends Microbiol. 2003; 11:69–73. [PubMed: 12598128]

110. Murad AM, Lee PR, Broadbent ID, Barelle CJ, Brown AJ. CIp10, an efficient and convenient integrating vector for *Candida albicans* . Yeast. 2000; 16:325–327. [PubMed: 10669870]

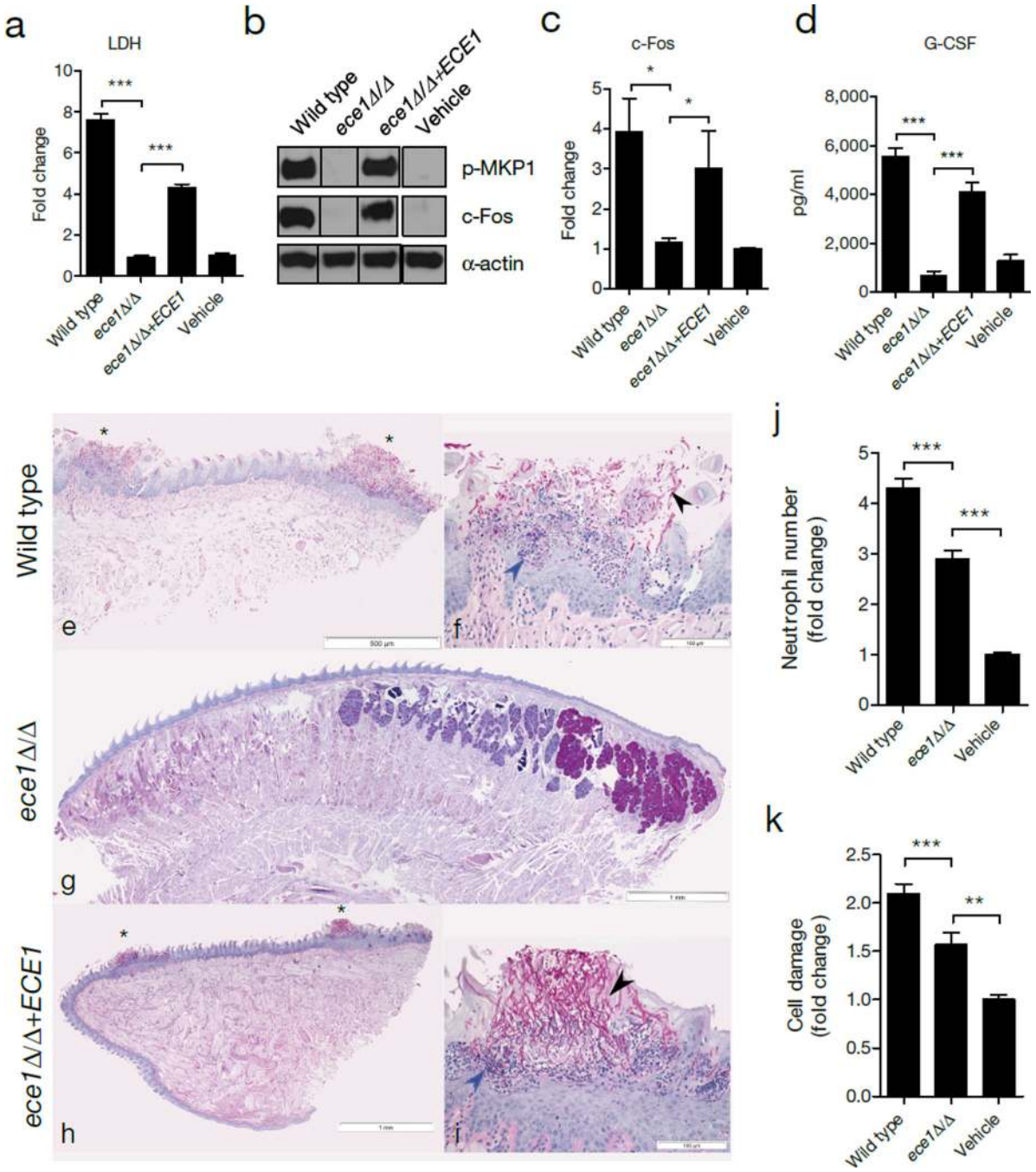

Figure 1. *ECE1* is required for epithelial activation and *C. albicans* infection

TR146 cells were infected with the indicated *C. albicans* strains. **(a)** LDH release 24 h post-infection (p.i.) (MOI = 0.1). **(b)** Induction of p-MKP-1 and c-Fos at 2 h p.i. (MOI = 10). **(c)** c-Fos DNA binding at 3 h p.i. (MOI = 10). **(d)** G-CSF production at 24 h p.i. (MOI = 0.01). **(e-i)** PAS-stained tongues from mice subjected to OPC 2 d p.i. **(e, g, h)** Whole-mount (x25) and **(f, i)** high-power (x200) views of PAS-stained tongues of mice infected with *C. albicans* wild type (**e, f**), *ece1*Δ/Δ (**g**) and *ece1*Δ/Δ+*ECE1* (**h, i**). Invading hyphae (black arrow) and inflammatory cells (blue arrow) are indicated. **(j)** Quantification of neutrophils in zebrafish

swimbladder following infection with wild type *C. albicans* (n (number of fish) = 47), *ece1*Δ/Δ (n = 53) or PBS (n = 40). **(k)** Quantification of damaged cells in zebrafish swimbladder after infection with *C. albicans* wild type (n = 73), *ece1*Δ/Δ (n = 59) or vehicle (n = 63). Data are representative **(b, e-i)** or the mean **(a, c-d, j-k)** of three biological replicates. Error bars ± SEM. Data were analyzed by one-way ANOVA (**a, d**), paired T test (**c**) or Kruskal-Wallis (**j, k**) and * = $P < 0.05$, ** = $P < 0.01$, *** = $P < 0.001$. For gel source data, see Supplementary Figure 1.

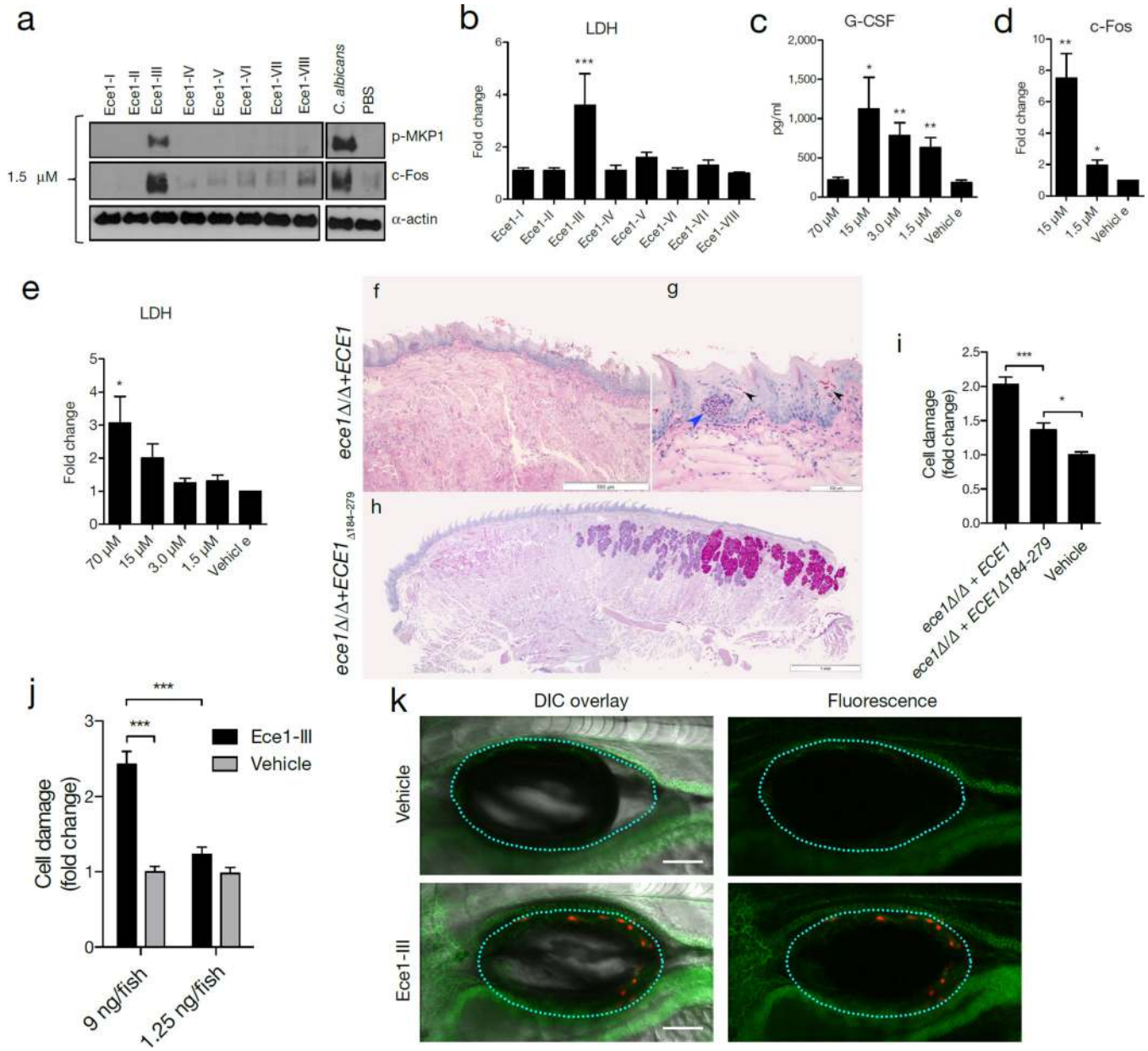

Figure 2. Ece1-III$_{62–93}$ is the active region of Ece1p and is required for TR146 cell activation and mucosal *C. albicans* infection

(a) Induction of p-MKP-1 and c-Fos 2 h post-stimulation (p.s.) with Ece1 peptides at 1.5 µM. **(b)** LDH release 24 h p.s. with 70 µM Ece1 peptides. **(c)** Induction of G-CSF 24 h p.s. with Ece1-III$_{62–93}$ **(d)** c-Fos DNA binding induction 3 h p.s. with sub-lytic concentrations of Ece1-III$_{62–93}$ **(e)** LDH release 24 h p.s. with Ece1-III$_{62–93}$ **(f-h)** PAS stained tongue sections from mice subjected to OPC, 2 d p.i. with **(f, g)** *C. albicans ece1Δ/Δ+ECE1* (x25 and x200) or **(h)** *ece1Δ/Δ+ECE1$_{Δ184–279}$*. Invading hyphae (black arrows) and infiltrating inflammatory cells (blue arrow) are shown. **(i)** Damaged cells in a zebrafish swimbladder 24 h p.i. with *C. albicans ece1Δ/Δ+ECE1* (n (number of fish) = 44), *ece1Δ/Δ+ECE1$_{Δ184–279}$* (n = 58) or vehicle (n = 58). **(j)** Damaged cells in zebrafish swimbladders after stimulation with 9 ng (n

= 51) or 1.25 ng (n = 56) Ece1-III$_{62–93,}$ or vehicle (40% DMSO, n = 54 and 5% DMSO, n = 55). **(k)** Co-localization of adherens junctions (α-catenin-citrine) with Ece1-III$_{62–93}$-damaged cells (Sytox Orange-positive cells) in a zebrafish swimbladder. Data are representative **(a, f-h, k)** or mean **(b-e, i-j)** of three biological replicates **(a-d)** or ten mice or fish **(f-h, k)**. Error bars show ± SEM. Data were analyzed by one-way ANOVA (**b, c, e**) paired T test (**d**) or Kruskal-Wallis (**i, j**). * = $P < 0.05$, ** = $P < 0.01$, *** = $P < 0.001$ (compared with vehicle control unless otherwise indicated). For gel source data, see Supplementary Figure 1.

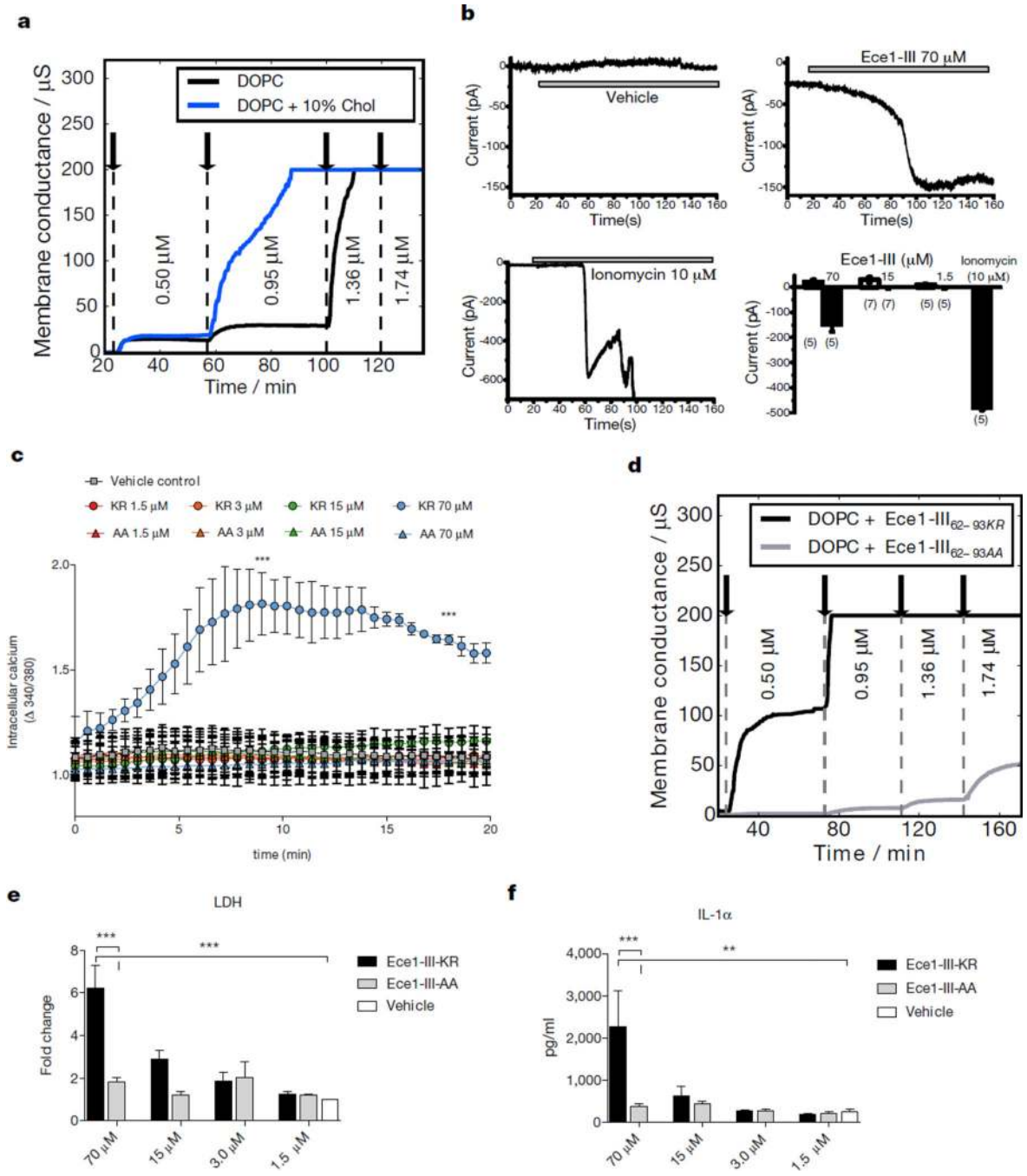

Figure 3. Ece1-III$_{62–93}$ functions as a cytolytic peptide toxin

(a) Kinetic changes in conductance of tethered lipid membranes after exposure to different concentrations of Ece1-III$_{62–93}$. **(b)** Evoked inward current at a membrane potential of −60 mV in TR146 cells post-addition of Ece1-III$_{62–93}$ or ionomycin (positive control); individual (representative) and cumulative changes (bar chart - number of cells analyzed below each bar) shown. **(c)** Intracellular calcium level kinetics in TR146 cells post-stimulation (p.s.) with Ece1-III$_{62–93}$ wild type (Ece1-III$_{62–93KR}$) or Ece1-III$_{62–93}$ AA C-terminal substitution (Ece1-III$_{62–93AA}$). **(d)** Kinetic changes in conductance of tethered DOPC membranes after

exposure to different concentrations of Ece1-III$_{62–93KR}$ and Ece1-III$_{62–93AA}$. **(e)** LDH release and (**f**) Secretion of IL-1α from TR146 cells 24 h p.s. with Ece1-III$_{62–93KR}$ or Ece1-III$_{62–93AA}$. Data shown are representative **(a, d)** or mean **(b-c, e-f)** of three biological replicates. Error bars show ± SEM. Data were analyzed by one-way ANOVA (**c, e** and **f**). ** = $P < 0.01$, *** = $P < 0.001$.

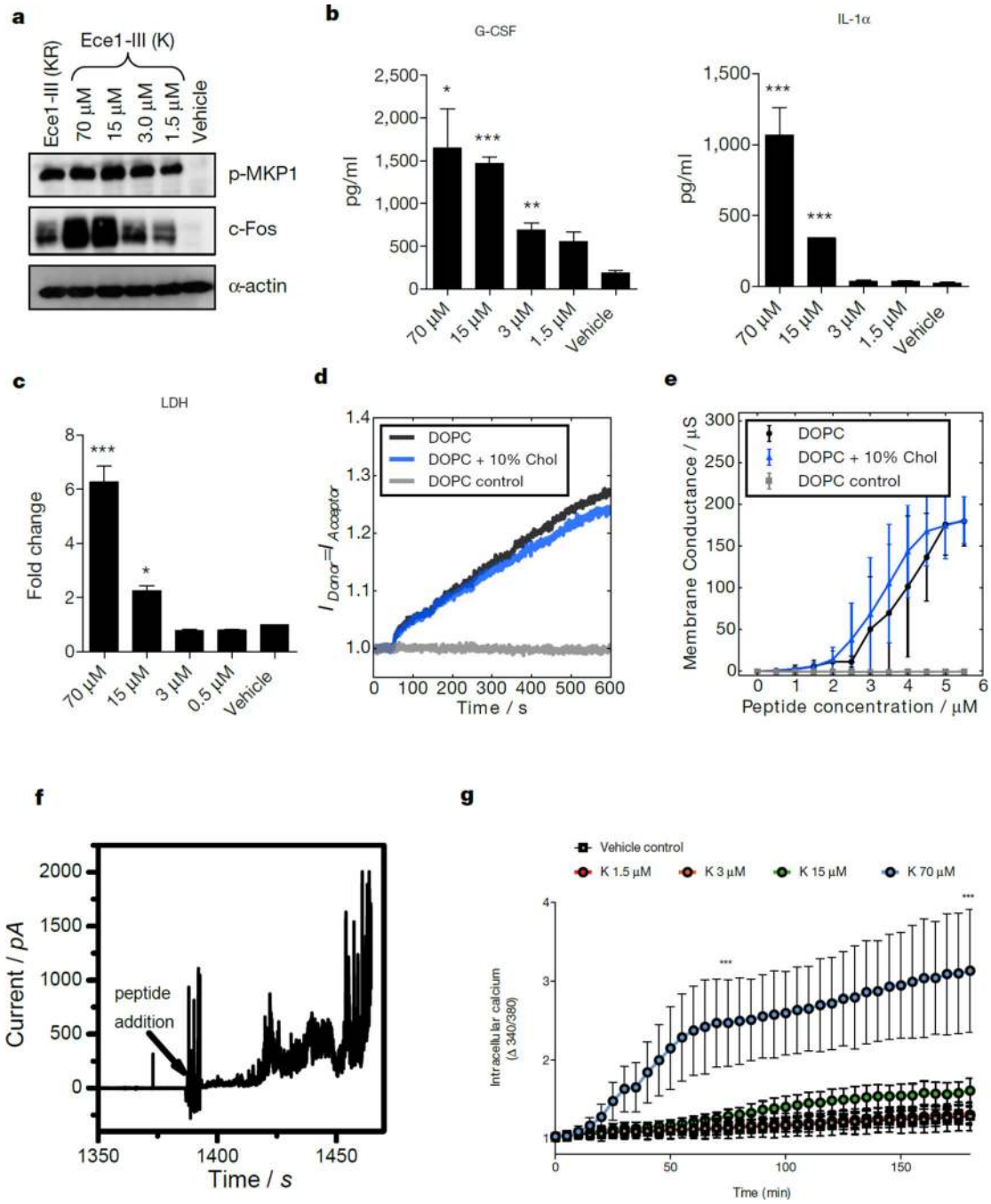

Figure 4. Ece1-III$_{62–92K}$ functions as a cytolytic peptide toxin that activates and damages epithelial cells

(a) Induction of p-MKP-1 and c-Fos 2 h post-stimulation (p.s.), and **(b)** secretion of G-CSF and IL-1-α 24 h p.s., and **(c)** LDH release 24 h p.s. of TR146 cells with Ece1-III$_{62–92K}$. **(d)** Förster resonance energy transfer (FRET) showing intercalation of Ece1-III$_{62–92K}$ (10 μM) into lipid liposomes. **(e)** Average peptide concentration-dependent changes in conductance of tethered lipid membranes. **(f)** Ece1-III$_{62–92K}$ (4 μM) induced permeabilization of planar lipid membranes showing heterogeneous and transient lesions leading to membrane rupture.

(g) Intracellular calcium level kinetics in TR146 cells p.s. with Ece1-III$_{62–92K}$. Data shown are representative **(a, d, f)** or mean **(b-c, e, g)** of three biological replicates. Error bars show ± SEM. Data are analyzed by one-way ANOVA (**b, c**). * = $P < 0.05$, ** = $P < 0.01$, *** = $P < 0.001$ (compared with vehicle control). For gel source data, see Supplementary Figure 1.